UNIVERSITÀ DEGLI STUDI DI CAMERINO

School of Advanced Studies

DOCTORAL COURSE IN

CHEMICAL AND PHARMACEUTICAL SCIENCE

AND BIOTECHNOLOGY

XXXVI cycle

TITLE THESIS

GABAERGIC MIR-34A REGULATES DORSAL RAPHÈ INHIBITORY TRANSMISSION IN RESPONSE TO AVERSIVE, BUT NOT REWARDING, STIMULI

PhD Student
Serafina Manila Guzzo

Supervisor
Carlo Cifani

Co- supervisor
Diego Andolina

Abstract

The survival of an organism relies on the processing of both positive and negative valence stimuli, leading to appropriate behavioral responses. Dysregulation of neural circuits involved in encoding stimuli with diverse valences contributes to various psychiatric disorders. The Dorsal Raphe Nucleus (DRN) actively participates in diverse behaviors and orchestrates emotional responses to both rewarding and aversive experiences. Serotonin (5HT) plays a crucial role in stress and reward responses, with its regulation intricately linked to GABAergic neuronal populations. Significantly, microRNA expression in the mammalian brain manifests distinct tissue and neuronal specificity, implying a potential involvement in cellular and circuit-level functionality. Despite this observation, the complete comprehension of such specificity remains an ongoing endeavor.

Our findings indicate that acute exposure to aversive (restraint stress) and rewarding (chocolate) stimuli leads to a reduction in local GABA release within DRN. Within the murine ventrolateral DRN, our study identifies a GABAergic subpopulation expressing microRNA-34a (miR-34a). Surprisingly, miR-34a exclusively modulates GABA release only under aversive conditions. Notably, inhibiting miR-34a selectively impairs the capacity to cope with real contingent threats, while leaving behaviors related to risk assessment, positive valence stimuli, and cognitive performance unaffected.

Additionally, our investigation reveals a correlation between miR-34a levels in GABAergic neurons in the DRN and plasma miR-34a levels. These results strongly suggest that plasma miR-34a level can represent a biomarker for miR-34a level on GABAergic neurons in the DRN.

These findings propose that microRNAs, such as miR-34a, could function as a comprehensive signature for specific neural subpopulations exhibiting valence-specific activity in the brain.

Preface

This doctoral thesis was carried out in the laboratories of Psychobiology of Behavior at Sapienza University of Rome, where a collaborative environment was instrumental in its execution.

I am pleased to include a publication stemming from this research within the thesis, titled "GABAergic miR-34a regulates Dorsal Raphè inhibitory transmission in response to aversive, but not rewarding, stimuli." This publication not only encapsulates a significant aspect of the findings but also serves as the primary source of the results and graphs incorporated into the broader scientific discourse.

The inclusion of these results enriches the thesis, highlighting the contributions of the conducted research. I extend my appreciation to all those involved in making this research endeavor and the resulting publication a valuable part of this doctoral work.

List of Abbreviations

CRFR1 (Corticotropin-Releasing Factor Receptor 1)

DLT (Dark-Light Test)

DRD (Dorsal Raphe Dorsal)

DRN (Dorsal Raphe Nucleus)

DRV (Dorsal Raphe Ventral)

DRVL (Dorsal Raphe Ventral Lateral)

FCT (Fear Conditioning Test)

FST (Swimming Test)

ISH (In Situ Hybridization)

LVT (Looming Visual Test)

mIPSCs (Miniature Inhibitory Post-Synaptic Currents)

miRNAs (MicroRNA)

mPFC (Medial Prefrontal Cortex)

NORT (Novel Object Recognition Test)

OFT (Open Field Test)

PFA (Paraformaldehyde)

PFC (Prefrontal cortex)

SIT (Social Interaction Test)

SPT (Saccharin Preference Test)

5-HT (Serotonin)

VTA (Ventral Tegmental Area)

1. Introduction

1.1 The Dorsal Raphe Nucleus (DRN)

The DRN is a bilateral and neurochemically heterogeneous nucleus located within the ventral periaqueductal gray (Michelsen et al., 2007). The DRN exhibit distinct anatomical subdivisions, namely the dorsal (DRD), ventral (DRV), and ventrolateral (DRVL) parts. The phylogenetic conservation of raphe nuclei across various vertebrate species emphasizes their evolutionary significance, demonstrating remarkable conservation of both structure and function across different evolutionary stages (Ngeles Fernández-Gil et al., 2010).

The DRN constitutes a primary source of neuromodulators in the central nervous system (CNS), encompassing approximately one-third of all serotonergic neurons (5-HT neurons) in human brain (J. Chen & Condron, 2008; Hornung, 2010). These strategically arranged neurons along the midline play a crucial role in neurotransmission, innervating cortical and limbic projection areas in a topographically organized manner (Calizo et al., 2011; Commons, 2020). These projections include the cerebral cortex, caudate-putamen, substantia nigra, nucleus accumbens, ventral tegmental area (VTA), thalamus, lateral and medial habenula, hypothalamus, hippocampus, and amygdala (Beliveau et al., 2015; Peyron et al., 1997; Pollak Dorocic et al., 2014).

Preclinical studies have showed DRN serotonergic neurons respond to both reward and aversive stimuli, adding complexity to their functional roles (Hayashi et al., 2015; Kawai et al., 2022). For instance, gain- and loss-of-function experiments suggest that amygdala-projecting DRN 5-HT neurons play a role in promoting anxiety-like behavior (Ren et al., 2018) and literature reports a significant correlation between 5-HT levels in the forebrain and specific behavioral responses (Deakin & Graeff, 1991), where elevated 5-HT levels favor pausing and waiting (Marcinkiewcz et al., 2016; Miyazaki et al., 2014), while reduced 5-HT levels promote impulsivity and perseverative responses in mice (Clarke et al., 2004; Harrison et al., 1997). The medial prefrontal cortex (mPFC) emerges as a prominent recipient of projections from the rostral and central subregions of the DRN (Chandler et al., 2013; Sargin et al., 2019). Mouse studies have observed that the

DRN-mPFC circuit strongly influences coping responses, where the increase of 5-HT firing promotes passive coping behavior during inescapable stressors such as the Forced Swimming Test (Amat et al., 2005; Andolina et al., 2013) commonly employed as a behavioral model to assess despair in mice.

Additionally, VTA DA neurons, classically implicated in reward processing, receive input from serotonergic neurons in the DRN, establishing the DRN as one of the largest sources of input to the VTA. These 5-HT projections play a crucial role in shaping the VTA's responses to positive stimuli and are integral to the interplay between the serotonergic and dopaminergic systems in reward processing (Beier et al., 2015; Cardozo Pinto et al., 2019; Ogawa et al., 2014).

Although the DRN show the highest density 5-HT, they demonstrate considerable heterogeneity in neuronal cell subtypes. About 25%–30% of the DRN comprises GABAergic neurons(Hernández-Vázquez et al., 2019), predominantly located in the DRVL region. This topographic distribution has functional consequences, as lateral GABAergic neurons inhibit 5-HTergic neurons in the central region (Challis et al., 2014).

GABAergic neurons significantly influence the excitability of DRN 5-HT neurons and 5-HT release in various brain regions (L. Zhou et al., 2017).

Consistently, studies in rodents have demonstrated that DRN GABAergic transmission plays a key role in mediating responses to both aversive and rewarding stimuli (L. Huang et al., 2017a; Y. Li et al., 2016; Seo et al., 2019; Spoida et al., 2014). Electrophysiological evidence (Rompre & Miliaressis, 1985) and pharmacological studies targeting DRN GABA/5-HT signaling have demonstrated the involvement of the DRN in reinforcement (Fletcher et al., 1993; Land et al., 2009; Shin & Ikemoto, 2010). When mice consume freely available food or sucrose, DRN 5-HT neurons are activated while GABAergic neurons are inhibited (Y. Li et al., 2016). Moreover, perturbation of GABAergic transmission within the DRN has been associated with the stress response and anxious behavior (Challis et al., 2013; L. Kirby, 2000). During stressful conditions, the local firing of these interneurons is heightened due to the stimulation of Corticotropin-Releasing Factor Receptor 1

(CRFR1) receptors, a stress hormone receptor recognized for its expression on GABAergic neurons (L. G. Kirby et al., 2008).

Furthermore, the intricate interplay between GABAergic and 5HT modulation in the DRN significantly shapes the expression of defensive responses to stimuli (Seo et al., 2019). How an individual responds to approaching threats is influenced by the dynamic interaction of sensory inputs from various modalities with underlying neurotransmitter systems (Barbano et al., 2020; Z. Li et al., n.d.; Shang et al., 2018). Recent studies in mice have provided insight into the interaction of stimuli within the visual sensory system. These studies reveal that retinal ganglion cells projecting to the DRN activate GABAergic neurons within the DRN. This activation, in turn, leads to the inhibition of serotonergic neurons during looming-evoked defense responses (Huang et al., 2017). This reciprocal interaction within the DRN not only fine-tunes responses to stimuli, but GABA-related neural dynamics also appear to be selective for stimulus valence. Neural dynamics associated with movement in response to positive and negative environments show opposing GABAergic modulations, indicating that DRN circuits undergo a switch between distinct operational modes to facilitate environment-specific adaptive behaviors (Seo et al., 2019).

1.2 MicroRNA (miRNAs)

In 1993, Victor Ambros's lab identified lin-4 in Caenorhabditis elegans, unveiling microRNAs as key gene regulators (R. C. Lee et al., 1993). miRNAs constitute a class of endogenous noncoding RNAs, typically 19 to 25 nucleotides in length, exerting precise control over gene expression in various biological processes. Although miRNAs make up only 1-2% of the human genome, they influence approximately 30% of coding genes in complex ways (Filipowicz et al., 2008). These miRNAs, identified across species with conserved mRNA sequences, suggest the possibility of gaining insights into human functions and mechanisms through studies of model organisms (Friedman et al., 2009).

The miRNA biogenesis pathway is responsible for processing pre-miRNAs into mature miRNAs. The first transcribed product is a long non-coding RNA named pri-miRNA, which is cut by Drosha endonuclease, an enzyme with two RNAse III domains. Drosha cuts one strand of the stem of the pri-miRNA hairpin, which produce a 60-110 nucleotides stem-loop called pre-miRNA (Lee et al., 2003; Zeng & Cullen, 2003). Pre-miR is polyadenylated to gain more stability and then exported to cytoplasm by Exportin 5 and RAN–GTP (Griffiths-Jones, 2006; Lee et al., 2003). The pre- miRNA is further processed by Dicer, an endonuclease which cuts both hairpin's strands near the loop to generate the miRNA duplex (Bhattacharya et al., 2017). After processing, miRNAs form the RNA-induced silencing complex (RISC), which carries out post-transcriptional regulation by binding to the complementary 3'UTR region of messenger RNA (mRNA) via their seed region (Bartel, 2004; Filipowicz et al., 2008; Ha & Kim, 2014).

In the field of neurobiology, miRNAs play a fundamental role in neuronal development and the mature functions, influencing processes such as differentiation, proliferation, neurite growth, neurogenesis, synaptic plasticity, and memory (Ashraf et al., 2006; Y. Chen et al., 2022; McCall et al., 2017; Y. Wang et al., 2007). Their spatially specific expression in neuronal axons and dendrites enables synaptic modulation in response to environmental stimuli (Bicker et al., 2013; Lugli et al., 2008).

Recent studies have unveiled distinct miRNA expression patterns in specific neuronal populations, indicating a preference for γ-aminobutyric acid (GABA)ergic inhibitory neurons or glutamatergic excitatory neurons (He et al., 2012). Moreover, the expression and functions of miRNAs play a crucial role in shaping the developmental pathways of specific GABAergic interneuron populations (Lichtensteiger et al., 2021; Taylor et al., 2023). Dysregulation of miRNAs in GABAergic interneurons is implicated in neurodevelopmental disorders, emphasizing their significance in maintaining stable and functional neural circuits, influencing the physiological characteristics and organization of mature brain networks (Strobl-Mazzulla - 2012, n.d.; Tuncdemir et al., 2015).

The complex connection between miRNAs and psychological well-being is evident with alterations in miRNA function associated with various psychiatric disorders, including anxiety (Fonken et al., 2016; Haramati et al., 2011), major depressive disorder (Lopez et al., 2014), post-traumatic stress disorder (Balakathiresan et al., 2014), bipolar disorder (Rong et al., 2011), and schizophrenia (Lai et al., 2011; Beveridge et al., 2010).

Genetic variations in miRNA expression play a significant role in shaping stress responses, and stress induces the expression changes of distinct miRNAs in a region-specific manner (Cohen et al., 2017; Zurawek et al., 2017). Moreover, different quantitative variations in miRNA expression have been observed in response to acute and chronic stress exposure, underscoring their dynamic involvement in molecular changes induced by stress (Meerson et al., 2010). In a mouse study, specific microRNAs were found to play a crucial role in regulating the motivational properties of drug addiction within the prefrontal cortex (PFC) and striatum following the self-administration of addictive drugs (Kenny, 2014). Beyond the boundaries of the brain, miRNAs have become the focus of studies as potential biomarkers in various diseases, including cancer, immune-related disorders, and infectious diseases (Mohamed et al., 2023; Nahand et al., 2019; S. Wang et al., 2015). In fact, their expression is not limited to the brain but extends to various tissues and body fluids such as blood plasma, serum, cerebrospinal fluid, urine, saliva, and tears (Sohel, 2016). MiRNAs, after being transcribed in the cellular nucleus, are actively transported from the nucleus to the cytoplasm, where they can be released into bodily fluids or selectively secreted in response to specific stimuli. Therefore, the noninvasive diagnosis and prognosis can be developed using circulating miRNAs (cimiRNAs). In Alzheimer's disease, a panel of seven plasma miRNAs (miR-545-3p, -301a-3p, -191-5p, -142-3p, -15b-5p, let-7g-5p, and let-7d-5p) exhibits a diagnostic accuracy of 95% for distinguishing individuals with Alzheimer's from healthy controls (Gupta et al., 2017). This high diagnostic precision has led to the development of various diagnostic tools, and ongoing clinical trials are exploring their potential application in pharmacological therapies (Chakraborty et al., 2021). In the realm of psychiatric disorders, the utilization of miRNAs as biomarkers represents an expanding area of research, demonstrating significant promise. For example, a study identified a panel of miRNAs in serum

that showed potential in diagnosing depression (Maffioletti et al., 2014). Similarly, a recent case-control study, conducted on serum samples, revealed promising outcomes by identifying a panel of three miRNAs (miR-16, miR-135a, and miR-1202) in 39 depressed patients, suggesting that this miRNA panel could enhance diagnostic accuracy for depression compared to the use of single miRNAs (Gheysarzadeh et al., 2018). Additionally, recent research associated a cluster of miRNAs (miR-7-5p, miR-23b-3p, miR-142-3p, miR-221-5p, and miR-370-3p) with Bipolar II Disorder (S. Y. Lee et al., 2020).

These findings highlight the potential of miRNAs as diagnostic and prognostic biomarkers in psychiatric disorders, with the implications for predicting treatment response. Notably, the analysis of circulating miRNAs presents a promising alternative for diagnosis, offering an objective and potentially more sensitive approach compared to traditional methods reliant on questionnaires and behavioral assessments (Gururajan et al., 2016).

1.3 MicroRNA-34 (miR-34)

MiR-34a is a crucial member of the miR-34 family, which encompasses independently encoded miR-34a and co-transcribed miR-34b/miR-34c. These miRNAs play critical roles in various neurobiological processes within the CNS, impacting brain development (Jauhari et al., 2018) and contributing to pathological conditions, including neurological diseases (Latta et al., 2015; Zhao et al., 2019).

Numerous studies suggest the central involvement of the miR-34 family in the regulation of the stress response (Andolina et al., 2016; Haramati et al., 2011). Clinical investigations have reported modulation of this miRNA-34 family in the serum, cerebrospinal fluid, and neural tissues of patients diagnosed with major depression (Azevedo et al., 2016; Smalheiser et al., 2012; Wan et al., 2015) and in response to chronic antidepressant treatment (Bocchio-Chiavetto et al., 2013; Kuang et al., 2018).

Consistently, behavioral studies in mouse have demonstrated that genetic deletion of miR-34a/b/c (TKO mice) show an absence of behaviors mediated by fluoxetine in response to adverse conditions. This emphasizes the fundamental role of miR-34 not only in the stress response but also in behavioral responses to pharmacological treatments through the regulation of serotonin 2C (5-HT2C) receptor expression in DRN (Lo Iacono et al., 2021).

Preclinical studies using TKO mice revealed that this family of miRs control the amygdala-GABAergic mPFC-5-HT circuit in response to acute stress exposure, providing direct evidence that miRs regulate neurotransmission in vivo (Andolina et al., 2016; 2018).

Research indicates that miR-34a/b/c share only 20% of their targets, suggesting unique genetic regulations for individual miR-34 family members (Navarro & Lieberman, 2015). Studies have associated miR-34b and miR-34c with dopaminergic neuronal differentiation (De Gregorio et al., 2018), while miR-34b is involved in apoptosis of hippocampal astrocytes (Liu et al., 2016).

MiR-34a, characterized by a somatodendritic distribution, governs synaptic protein targets, contributing to the development of synaptogenesis (Agostini, Tucci, Steinert, et al., 2011). Notably, miR-34a appears to regulate stress-induced neurotransmission in the DRN and mPFC-amygdala downstream, potentially through its target CRFR1 (Lo Iacono et al., 2020). Additionally, it has been observed that miR-34a is highly expressed in the DRN (Andolina et al., 2018), where its recruitment is necessary to induce depressive-like behavior following chronic stress exposure (Lo Iacono et al., 2020).

Interestingly, miR-34a expression has been identified in the cerebellum GABAergic neurons during the embryonic stage in the mouse (He et al., 2012).

2. Experimental Hypothesis

The brain employs distinct circuits to encode positive and negative experiences driven by rewarding or aversive stimuli (Luo et al., 2015; Ren et al., 2018; Seo et al., 2019a). An important challenge lies in distinguishing different neuronal subpopulations and, consequently, the distinct mechanisms involved in coding such experiences, particularly when these are localized within the same circuit or brain area. Neuronal identity and physiology are guided by specific transcriptional profiles, including the selective expression of miRNAs. Indeed, miRNA expression often exhibits neuronal and sub-neuronal specificity, indicating a selective role in cellular function.

However, this specificity has yet to be fully leveraged for research or therapeutic purposes. With its pronounced expression in DRN (Andolina et al., 2018), miR-34a regulates mRNAs target, including CRFR1 and 5-HT2C receptors predominantly found in GABAergic neurons of DRNs (Homberg & Contet, 2009; Spoida et al., 2014).

The project aims to fill a critical gap in our understanding of the mechanisms underlying the coding of experiences with opposite valences. The primary goal of this project is to explore the functional role of miRNAs within the specific neuronal populations where they are expressed and to ascertain whether they actively contribute to the regulation of valence-specific motivated behaviors. We aim to explore whether miR-34a orchestrates the response of populations of GABAergic neurons, selectively responsible for processing negatively valence stimuli in the DRN. Additionally, given the detectability of miRNA-34a in plasma and their potential as biomarkers, understanding the correlation between changes in plasma miRNA levels and alterations in specific neural populations becomes a crucial avenue of investigation.

Hypothesis 1: miR-34a is selectively expressed in GABAergic neurons within the DRN. Approach: we combined in situ hybridization (ISH), miRNAscope ISH, and immunofluorescence for spatial and cellular analysis of miR-34a expression in the mouse brain.

Hypothesis 2: miR-34a mediates GABAergic control of serotonergic DRN neurons in response to valence-specific stimuli. Approach: we employed electrophysiological and microdialysis approach to measure GABAergic activity in the DRN in response to negative and positive valence stimuli following miR-34a inhibition.

Hypothesis 3: GABAergic miR-34a in the DRN is selectively involved in the behavioral response to specific valence experiences. Approach: we performed a comprehensive behavioral characterization of mice undergoing pharmacological inhibition of miR-34a in the DRN.

Hypothesis 4:
Plasmatic miR-34a originates from DRN GABAergic neurons. Approach: We evaluated plasmatic miR-34a following modulation of miR-34a in the DRN and in GABAergic neurons.

3. Materials and methods

3.1 Animals

In all experiments, male mice aged 12-15weeks were used. C57BL/6 mice were obtained from Charles River Laboratories, Italy. Conditional miR-34 a/b/c knockout mice (miR-34a$^{loxP/loxP}$) were kindly provided by Alexander Yu. Nikitin from the Department of Biomedical Sciences and Cornell Stem Cell Program, Cornell University, Ithaca, NY (Cheng et al., 2014). TKO mice for all three members of the miR-34 family have been kindly provided by Dr. Ventura (Memorial Sloan Kettering Cancer Center, NY, USA), (Concepcion et al., 2012). Gad2::Cre mice were supplied by Cornelius Gross (European Molecular Biology Laboratory, Monterotondo, Italy). The mouse model for the genetic selective knockdown of miR-34a in GABAergic neurons (Gad2::Cre/miR-34a$^{loxP/loxP}$) was generated by crossing Gad2::Cre with miR-34a$^{loxP/loxP}$ mice. All mice used in the experiments were bred on a C57BL/6 background. Upon weaning, the mice were housed in groups of 3 to 4 individuals per cage. They were maintained in a climate-controlled setting at a temperature of 21°C and subjected to a 12-hour light/dark cycle. Food and water were provided without restrictions. All experiments were conducted in accordance with the Italian national law (DL 26/2014) based on the European Community Council Directive (2010/63/UE). The experimental procedures on animals were approved by the Italian Ministry of Health (no. 769/2017 and 70/2022).

3.2 In Situ Hybridization

ISH was conducted on coronal slices of the DRN of WT, Gad2::Cre, miR-34a$^{loxP/loxP}$ and Gad2::Cre/miR-34a$^{loxP/loxP}$ mice. Brains were collected, promptly frozen in optimal cutting temperature (OCT) compound, sectioned cryogenically at a thickness of 20 μm, and affixed onto Superfrost Plus slides. The ISH procedure used a locked nucleic acid (LNA) probe for miR-34a (sequence: ACAACCAGCTAAGACACTGCCA) with a digoxigenin (DIG) label (Exiqon). For negative control purposes, hybridization was performed using a scrambled

LNA probe. The non-coding sequence is composed of a random assortment of vector bases.

Briefly, the sections were initially fixed using 4% paraformaldehyde (PFA), subjected to proteinase K digestion for 5 minutes, acetylated, and subsequently subjected to hybridization with the respective probes. The hybridization solution consisted of 50% formamide, 5× saline-sodium citrate (SSC), 5× Denhardt's solution, 500 μg/ml salmon sperm DNA, and 250 μg/ml tRNA, and the hybridization was conducted overnight at 50°C. Following this step, post-hybridization washes were performed utilizing 50% formamide and 2× SSC at 45°C, followed by 2× SSC at room temperature. Sections were blocked and incubated overnight with anti-DIG-AP (Roche; at 1:1000). Signal detection was achieved using an NBT/BCIP substrate. The resultant images were captured using an Olympus BX53 microscope (with a 4X objective and a 1.25 numerical aperture). For quantitative analysis, ImageJ software was employed (Abràmoff, n.d.), and this analysis was conducted by an experimenter blind to the experimental groups of the animals. The miR-34a positive cells were enumerated in three sections that were sampled to encompass the entire rostro-caudal range of the nucleus.

3.3 MiRNAscope™

The miRNAscope™ procedure (Advanced Cell Diagnostic, USA) was executed following the manufacturer's guidelines, as outlined in reference (F. Wang et al., 2012). Briefly, C57BL/6 mice were deeply anesthetized and subsequently subjected to perfusion with a saline solution (0.9% NaCl) and 4% PFA. Following an overnight post-fixation in 4% PFA, the brains were immersed in a sucrose solution (30%) for cryoprotection, and then stored at a temperature of -80°C. Coronal slices with a thickness of 15 μm were achieved via a cryostat and were positioned on Superfrost Plus slides. The protocol involved dehydration, post-fixation, peroxidase application, and antigen retrieval. The miR-34a probe (SR-mmu-miR-34a-5p-S1, catalog number MIMAT0000542) was administered to the sections, and the amplification cascade was executed according to the manufacturer's instructions, with detection facilitated by Fast Red solution. Before the miRNAscope procedure,

the sections underwent an incubation step with primary antibodies, which included rabbit anti-GAD67 antibody (1:200; catalog number GXGTX101881, Genetex) and goat anti-5-HT antibody (1:400; catalog number ab66047, Abcam), all conducted in 0.1M phosphate buffer (PB) with 0.3% Triton X-100. After the miRNAscope protocol, the sections were treated with secondary antibodies—Alexa Fluor 647 donkey anti-rabbit IgG and Alexa Fluor 488 donkey anti-goat IgG (both at 1:200; Molecular Probes; Eugene, OR, USA; catalog number A31572)—for 1 hour at room temperature (RT). After air-drying, the sections were covered with GEL/MOUNT (Biomeda, Foster City, CA, USA) and examined using a confocal laser-scanning microscope (Leica SP5).

For quantitative analysis of GAD67/miR34a and 5-HT/miR34a co-localization, images were acquired using a 20× objective with a 0.07 zoom factor with confocal microscope. All neurons that exhibited double labeling in three sections, evenly distributed across the caudo-rostral extent of the nucleus, were counted. To assess cellular co-localizations, double immunolabeled neurons were evaluated by counting and characterizing their labeling through the proprietary image analysis program of the Leica confocal microscope (Leica LSM software). Digital images from the same optical section were acquired for each laser channel (green/blue and red) and merged to create a third image for cell counting. The characteristics of immunolabeled cells were analyzed by zooming in on the cells and sequentially excluding each channel to enhance the visualization of cellular morphology. All quantitative analyses were conducted in a blinded manner with respect to the experimental group of the animals.

3.4 Stereotaxic surgery

The mice were subjected to anesthesia using Zoletil 100/Rompun 20, following which they were positioned within a stereotaxic frame (manufactured by David Kopf Instruments, Tujunga, CA, USA) outfitted with a dedicated mouse adapter. The coordinates for all experimental interventions were derived from the reference “The Mouse Brain in Stereotaxic Coordinates" (*Themousebraininstereotaxiccoordinates*, n.d.).

3.4.1 Intra-DRN antagomir-34a (Ant-34a) infusion

AntagomiR-34a, specifically, LNA Antimir-34 (15-mer) with the sequence 5'-3' ACGTCTATACGCCCA (manufactured by Qiagen), along with a negative control sequence, was administered within the DRN of C57BL/6 mice through a 26-gauge guide cannula. This cannula had been implanted 48 hours prior to the experiment, positioned at 1 mm from the DRN. During implantation, the following coordinates from the bregma were employed: anterior-posterior (AP) = +4.36 mm, medio-lateral (ML) = +1.5 mm, and dorso-ventral (DV) = +2.0 mm, at an angle of 26°.

For the condition involving restraint stress, Ant-34a or its corresponding negative control (0.5 µl at 10 µM concentration) was infused at a flow rate of 0.25 µl/min. This infusion was performed right before the onset of the stressful stimulus. In experiments assessing the impact of rewarding stimuli on GABA levels and in behavioral tests, Ant-34a or its negative control were infused 48 hours prior to the stimulus or test. This scheduling was designed to eliminate the confounding influence of immobilization-induced stress, as even the brief physical restraint required for infusion was demonstrated to induce significant stress. In our observations, this stress was adequate to alter GABA release in the DRN for at least 2 hours(Stuart & Robinson, 2015).

3.4.2 In vivo microdialysis

In Vivo Microdialysis Procedures: the procedures were performed on mice using vertical concentric dialysis probes made from AN69 fibers obtained from Hospal Dasco (Bologna, Italy). These probes were manufactured following established methods and protocols. Each probe had a total length of 3.5 mm, featuring a 1 mm long dialysis membrane and an external diameter of 0.24 mm and following coordinates were used: AP = + 4,36 mm, ML = + 1,5 mm, angled 26°. To facilitate unrestricted movement, the microdialysis probe was connected to a Fusion 740 pump sourced from KR Analytics Ltd. (UK) using PE-20 tubing and an ultralow-torque dual-channel liquid swivel (Model 375/D/22QM, Instech Laboratories, Inc., Plymouth Meeting, PA, USA). A constant flow rate of 2 µl/min was maintained,

with an artificial cerebrospinal fluid containing 147 mM NaCl, 1 mM MgCl, 1.2 mM CaCl2, and 4 mM KCl pumped through the dialysis probe.

Experimental Setup: the mice were accommodated in circular cages equipped with microdialysis apparatus and provided with familiar bedding. An acclimatization period of approximately 1 hour was observed before the commencement of baseline sample collection. Dialysate samples were collected at 20-minute intervals, with three samples taken during baseline measurements and six samples collected during conditions involving restraint or exposure to chocolate. The baseline concentration was determined based on the average of three samples taken immediately before treatment, ensuring a variation of less than 10%.

GABA Concentration Analysis: GABA concentrations in the collected samples, expressed in pg/20 µl, were analyzed using High-Pressure Liquid Chromatography (HPLC). An Alliace HPLC system equipped with a fluorescence detector (474 Model, Waters Corporation, Milford, MA) was employed for this purpose. Each sample underwent analysis prior to derivatization. Subsequently, a treatment involving 50 µl of o-Phthaldialdehyde (OPA) was applied, following established procedures (Rea et al., 2005). The mobile phase used for the HPLC process consisted of 70 mM disodium hydrogen phosphate, 400 µM EDTA, 0.15% (v/v) tetrahydrofurane, and 26% (v/v) methanol, with a pH of 5.25.

Experimental Timeline and Data Analysis: the microdialysis experiments were conducted 48 hours after the surgical procedure. The resulting GABA concentration values were presented as percentage changes from the mean baseline values, with both the mean and standard error of the mean (SEM) reported.

3.5 Ex-vivo electrophysiological recordings

3.5.1 Sample Preparation: mice were euthanized by decapitation, and their brains were extracted from the cranial cavity. The brains were dissected in a chilled oxygenated slicing solution containing the following concentrations (in mM): 234 sucrose, 26 NaHCO3, 11 glucose, 10 MgSO4, 2.5 KCl, 1.25 NaH2PO4, and 0.5 CaCl2, all saturated with a mixture of 95% oxygen and 5% carbon dioxide. Coronal

brain sections, each 250 μm thick and containing the DRN, were obtained using a vibratome (VT-1200S, Leica Biosystems, Germany). These brain slices were then incubated at 34 °C for 30 minutes for recovery and subsequently at room temperature (24 ± 1 °C) in an oxygenated artificial cerebrospinal fluid (ACSF) composed of (in mM): 126 NaCl, 26 NaHCO3, 10 glucose, 2.5 KCl, 2 CaCl2, 1.25 NaH2PO4, and 2 MgSO4. After this recovery period, the brain slices were transferred to the recording chamber for electrophysiological recordings.

3.5.2 Recording Procedure: neurons were visualized using an upright microscope (ECLIPSE E600FN, Nikon) equipped with a 60× water-immersion lens. Whole-cell patch clamp electrophysiological recordings were obtained from putative 5-HT neurons. Neurons were chosen based on their size, shape, and location within the DRN, with a preference for those located close to the midline. Once the whole-cell configuration was achieved, neurons were identified based on their firing patterns.

3.5.3 Distinctive Criteria for Neuronal Identification: for putative 5-HT neurons, characteristic features such as the "shoulder" of action potentials and an average half-width of 0.97±0.03 ms (n=46) were used for identification (Jin et al., 2015; Kirby et al., 2003; Marinelli et al., 2004). Other neurons, not identified as serotoninergic, had an average half-width of 0.67±0.05 ms (n=4). The presence of residual spikes after applying tetrodotoxin (TTX) was also checked to confirm the presence of calcium spikes. Only neurons exhibiting residual spikes post-TTX were included in the analysis.

3.5.4 Electrophysiological Data Collection: neurons were recorded using a MultiClamp700B amplifier and pClamp 10 software (Molecular Devices, USA). Data were filtered at 3 kHz and digitized at 10 kHz using a Digidata 1440 (Molecular Devices, USA). During recording, slices were submerged in oxygenated ACSF and perfused at 32–34 °C. Recording pipettes (3–5 MΩ) were filled with an internal solution (in mM: 70 K-gluconate, 70 KCl, 10 HEPES, 4 EGTA, 2 NaCl, 4 ATPMg, 0.3 GTP-Na, pH 7.26, 291 mOsm).

3.5.5 mIPSC Recording and Analysis: miniature inhibitory post-synaptic currents (mIPSCs) were recorded in voltage clamp mode at −70 mV. To block AMPA receptor-mediated post-synaptic currents and sodium channel-dependent action

potentials, DNQX (20 μM) and TTX (1 μM) were included, respectively. Series resistance was maintained below 25 MΩ, and recordings were excluded if the holding current exceeded −200 pA or if series resistance fluctuated by over 20% of the initial value. Offline analysis of mIPSCs was conducted using the Clampfit 10.7 software through a template search.

3.5.6 Post-hoc Identification: for post-hoc identification, neurons were filled with Alexa Fluor 488 (Thermofisher Scientific) via the recording pipette. Slices were subsequently transferred to 4% paraformaldehyde (PFA) and incubated overnight with an anti-5-HT antibody (Catalog No. 114-10207, RayBiotech) dissolved in 0.1M phosphate buffer (PB) and 0.3% Triton X-100. Following this, appropriate secondary antibody incubation and DAPI counterstaining (1:1000 for 5 minutes) were performed.

3.6 DRN activation by administration of aversive or rewarding stimuli

During the in vivo microdialysis experiments and before the ex-2ivo electrophysiology studies, we implemented a protocol that involves the application of restraint stress as a negatively valence stimulus. This protocol has been employed to elicit stress-induced physiological responses in animals by limiting their mobility (Cabib & Puglisi-Allegra, 1991). The containment apparatus comprises two main components. The former is designed to immobilize the animal's neck, thus limiting its freedom of movement. The latter is positioned at the base of the containment apparatus and located at a level corresponding to the animal's hips. Its U-shaped configuration effectively protects the animal's body, preventing it from assuming an upright position. The primary purpose of this containment apparatus is to create a stressful environment for the animal, characterized by limited freedom of movement, thus inducing a sense of confinement.

In microdialysis experiments, mice were restrained for 2 h to evaluate time-dependent changes induced by GABAergic outflow. In ex-vivo electrophysiology experiments the animals were subjected to the stress restriction procedure for 2 hours before being sacrificed. As a rewarding stimulus, we selected Milk chocolate

(Milka, Kraft) due to its established rewarding properties in a prior study (Patrono et al., 2015; Ventura et al., 2008). In all experiments, a portion of milk chocolate weighing 1 gram (Milka©: Fat = 29.5%; Carbohydrates = 58.5%; Proteins = 6.6%) was utilized as a palatable food source. The variables assessed included chocolate consumption and latency to consume. The animals were exposed to white chocolate for a duration of two hours, during which they were free to consume it. This exposure occurred both in the context of in vivo microdialysis and two hours prior to the initiation of ex-vivo electrophysiology recordings. To ensure that the mice were accustomed to the stimulus, a period of three consecutive days was designated for their pre-exposure to white chocolate. During this period, each day entailed a two-hour exposure session within their respective home cages. This familiarization process was conducted in advance of the scheduled microdialysis and electrophysiology experiments.

3.7 Tissue microdissection

Mice were euthanized through decapitation, and their brains, along with other organs, were extracted and preserved at -80°C. Tiny brain punches were obtained from coronal brain sections with a maximum thickness of 300 µm using a stainless-steel tube with a 1 mm internal diameter. The coordinates were determined in accordance with the Franklin and Paxinos brain atlas. In addition to the brain, specimens were collected from various organs, including testicles, thymus, adrenal glands, lungs, kidneys, heart, spleen, and plasma. Subsequently, these tissue samples were stored at -80°C until the day of analysis.

3.7.1 RNA Purification

Tissue RNA Extraction: The RNA extraction process involved an initial step using Trizol reagent (Thermo Fisher, Catalog Number: 15596026), wherein 800/900 µl of Trizol was utilized for 50 µg of tissue, and 1 ml of Trizol for 100 µg of tissue. This initial step was specific to organs. Subsequently, for both organs and other samples, the Total RNA Purification Plus Kit (Norgen Biotek, Thorold, Canada)

was employed following the manufacturer's instructions. RNA concentration was determined by measuring absorbance at 260 nm using a NanoDrop UV-Vis spectrophotometer. It is important to note that for organs, the initial Trizol step was exclusive to this sample type, while subsequent steps were consistent across all samples.

3.7.2 Tissue RNA Extraction

For brain structures, organs, and plasma, an equivalent amount of RNA (10 ng) underwent reverse transcription using the TaqMan MicroRNA Reverse Transcription kit (Applied Biosystems, Branchburg, NJ). Specific primer sets for miR-34a and the endogenous control sno135 (Taqman ID 000426 and 001230, Applied Biosystems) were employed. The cDNA templates (approximately 0.7 ng per sample) were subjected to qPCR using Taqman technology. Data were collected on the 7900HT thermal cycler apparatus equipped with SDS software version 2.3 (Applied Biosystems). Normalization to sno135 measurements and triplicate experiments were maintained, with results presented as fold changes (2^-ΔΔC(t)) following the ΔΔC(t) method (Schmittgen & Livak, 2008). Additionally, for normalization, miR-134, miR-16, and miR-212 (Taqman ID 001186, Taqman ID 462713_mat, Taqman ID 002551) were utilized as endogenous controls in tissues where sno135 showed variability. All samples underwent triplicate experiments to ensure data reliability.

3.8 Behavioral tests

The conducted behavioral tests, including the Forced Swim Test, Looming Test, Dark-Light Test, Open Field Test, Saccharin Preference Test, Social Interaction Test, Fear Memory Test, and Object Recognition Test, are integral components of this preclinical research. All experiments were performed on C57BL6 mice, and the role of miR-34a was investigated through the injection of Ant-34a in DRN. These tests were designed to offer valuable perspectives into the neural and psychological mechanisms underlying different aspects of behavior involving miR-34a.

These tests contributed to a more profound comprehension of the interconnectedness between these behaviors and the intricate neurobiological processes they are associated with. The tests were categorized into cognitive functions, positive valence, and negative valence, the latter to real threat and risk assessment. As a result, they established a crucial groundwork for investigating mental disorders underlying mechanisms of miR-34a.

All tests were conducted sequentially from the least to the most invasive, and a minimum interval of 24 hours between tests was maintained to decrease the chance that behavioral responses would be altered by prior test history.

3.8.1 Saccharin Preference Test (SPT)

The saccharin preference test was carried out as previously described with minor modifications (D'Addario et al., 2021). During the habituation day, the subjects were individually situated within a cage outfitted with two bottles, each containing 100mL of water. Following a duration of 24 hours, the subjects were subjected to a dual choice drinking evaluation, involving the presentation of two distinct options: a 1% saccharin solution (100mL) and regular drinking water (100mL). The quantification of intake was carried out with precision, allowing measurements accurate to the nearest 0.1 mL. Consistency was maintained by employing a uniform test cage configuration throughout the entire experimental procedure. Inclusion in the study was limited to mice demonstrating a minimum intake of 0.1 mL on the initial day. The outcomes were articulated in terms of a saccharin preference score, calculated as the ratio of saccharin solution intake to the sum of saccharin solution intake and water intake.

3.8.2 Social Interaction Test (SIT)

This test utilized a gray rectangular plexiglass apparatus measuring 60 × 40 × 24 cm in size. The apparatus consisted of a central starting chamber connected to two chambers, each containing a clear cylinder with an 8 cm diameter. The cylinders in

the apparatus were equipped with numerous small perforations, as previously detailed (Fiori et al., 2015). The testing procedure involved two sessions: a habituation session lasting 10 minutes and a test session also lasting 10 minutes. During the habituation session, mice were placed in the starting chamber and allowed to freely explore the entire apparatus. In the test session, a novel social stimulus, which was an age and sex-matched mouse, was placed in one cylinder, while a neutral object was placed in the other cylinder. To prevent potential bias, the positions of the social stimulus and the object were switched between the cylinders in each trial, and three different mouse as social stimulus were used to minimize habituation effects.

Mouse behavior during these sessions was recorded and the time spent by the mice interacting with each cylinder (social stimulus and object) was manually scored by a trained observer blind to treatment. The percentage of time spent in contact with the cylinders was then calculated using the formula: (time spent in social stimulus or object contact in seconds * 100 / (total time spent in social stimulus contact in seconds + total time spent in object contact in seconds).

3.8.3 Novel Object Recognition Test (NORT)

The experimental setup for the object recognition test comprised a circular open field, measuring 60 cm in diameter and 20 cm in height. Each mouse underwent three consecutive sessions on separate days, and at the conclusion of each session, the subject was returned to its home cage.

During the initial session (Open Field session), the mouse explored the central sector of the empty field for 5 minutes. In the subsequent session (Pre-test), the mouse was placed in the same sector of an open field containing two identical objects (A1 and A2: two identical cylinders of black plastic; 8 cm high and 4 cm in diameter, fixed horizontally to a rectangular base) and allowed to explore for 10 minutes.

On the final day, the objects were replaced for the Test session (10 min). One object remained identical to those in the previous session, while the other was a new object (a red and gray plastic coil; 8 cm high and 5 cm wide in diameter).

For the Open Field (OF) session, the Ethovision software automatically evaluated the distance moved (cm) and the time spent (sec) in different sectors of the device. Additionally, the time (sec) spent in contact with each of the two objects during the Pre-test and Test sessions was manually scored by an experimenter blind to the group of animals, using the Ethovision software. The recognition memory of the mice was further assessed by calculating the percentage of time spent with the familiar and novel objects during the Test session.

3.8.4 Fear Conditioning Test (FCT)

Mice were exposed to one day of fear conditioning and four consecutive days of conditioned fear extinction, adapted from previous work (Pibiri et al., n.d.). Briefly, the test was conducted in a conditioning chamber (25 cm × 19 cm × 17 cm) placed inside an illuminated, ventilated, and soundproof cabinet. The chamber was equipped with a grid floor (Coulbourn Modular Shock Floor) composed of 16 stainless steel rods (0.4 cm diameter) spaced 0.5 cm apart, linked to a shock generator (Coulbourn Precision Regulated Animal Shocker) that delivered an unconditioned stimulus shock (US). The US consisted of a scrambled foot shock (0.7 mA) delivered for 2 seconds through the bars.

The conditioned stimulus (CS) employed was a 2000 Hz pulsed tone generated by software at 80 dB. Stimulus delivery was controlled by an Arduino board connected to a GNU/Linux workstation. Video recording of the mice's behavior was conducted at 25 frames per second using a camera equipped with hardware MJPEG encoding, placed above the conditioning chamber.

On the training day, mice were introduced into the conditioning chamber and allowed to freely explore it. Two minutes after entry, a 30-second CS auditory signal was presented and co-terminated with a 2-second US foot shock. Subsequently, another CS-US pairing was performed after a 2-minute interval, and the mice were removed from the chamber 30 seconds following the conclusion of the US. To avoid olfactory cues, the conditioning chamber was cleaned with 70% ethanol between each mouse.

Over the next four days (extinction days), the context was altered by adding a white plastic panel (23 cm x 12 cm) in one corner of the chamber and a panel (18 cm x 17 cm) above the grid floor. During these days, only the CS stimulus was presented without the final two seconds of shock. The duration of freezing behavior (in seconds) was recorded during each trial as a measure of the animal's response.

3.8.5 Dark-Light Test (DLT)

DLT utilized a specialized apparatus comprising a rectangular box partitioned into two distinct environments: a dark area measuring 35×20×30 cm and a brightly illuminated compartment of the same dimensions. The two sections were connected by a narrow passage located centrally at the base of the partition. During a 5-minute recording period, the time spent and the number of entries into the aversive brightly lit compartment were meticulously recorded as part of the DLT assessment. DLT serves as an established tool to evaluate anxiety-related behavior in animals, particularly their preference for dark, sheltered areas over brightly illuminated, potentially aversive environments.

3.8.6 Forced Swimming Test (FST)

FST is an established experimental model widely used in behavioral studies to evaluate despair-like behavior in rodents (Lo Iacono et al., 2021). This test involves placing individual mice in a glass cylinder filled with water, maintained at a constant temperature of 28 ± 2°C. The water depth is set at 20 cm. For a period of 10 minutes the behavior of the mice is observed and recorded via a video surveillance system. An expert observer, unaware of the treatment of the animals, evaluates levels of immobility (reported in seconds) and swimming exhibited by the mice during this test.

3.8.7 Looming Visual Test (LVT)

LVT took place in a 40 cm × 40 cm × 40 cm experimental arena, where visual stimuli were projected using a ceiling-mounted computer monitor. A camera positioned adjacent to the monitor captured the mice's behavior.

To acclimate the mice and familiarize them with the environment, they were introduced to the arena for 10-minute sessions across two days. On the test day, before exposure to looming stimuli, the mice underwent a 5-minute habituation period.

Subsequently, three 'looming' stimuli were displayed. Each 'looming' stimulus initially showed a 5 cm black disk (equivalent to 2° of visual angle) that rapidly expanded to 25.5 cm (equivalent to 50° of visual angle) within 250 milliseconds, repeated 10 times. The expanded size was sustained for an additional 500 milliseconds, with a one-minute interval between each stimulus presentation.

This experimental design was inspired by previous studies (De Franceschi et al., 2016; Z. Zhou et al., 2019). The mice's responses, such as freezing or seeking shelter, were observed, and recorded. Video footage was analyzed using Ethovision motion tracking software.

3.9 Statistics

In the ISH experiment, the expression of DRN miR-34a in C57BL/6, miR-34a$^{loxP/loxP}$, Gad2::Cre, Gad2::C/miR-34$^{loxP/loxP}$ mice was analyzed by one-way ANOVA. Colocalization analysis between miR-34a/GAD-67 and miR-34a/5-HT was performed with a paired t-test.
In microdialysis experiments, the stability of GABA outflow under basal conditions (time points: −40, −20, 0) was assessed with a one-way repeated measures analysis of variance (ANOVA) within each group. GABA outflow levels in response to chocolate or stress, in naïve mice as well as Ant-34a/negative control infused subjects, were analyzed using a repeated-measures ANOVA with treatment (restraint stress vs chocolate, or Ant-34a vs. negative control) as the

“intermediate factor” and time as the “internal factor” (reference compared to 20, 40, 60, 80, 100 and 120 minutes from the start of the procedure). In all cases, the baseline was calculated as the average of the measurements at time points -40, -20, and 0. The basal extracellular GABA concentration in the DRN was analyzed by a t-test (2 groups: Ant- 34a vs negative control).

In electrophysiology experiments, a one-way Anova was used to compare the frequency and amplitude of mIPSCs from unstimulated, chocolate-exposed, and restraint-stressed naïve mice. A two-way ANOVA (treatment factor: Ant-34a and negative control; stimulus factor: no stimulus, chocolate-exposed, and restraint-stressed) was used to compare mIPSC frequency and neuron amplitude 5- HT registered.

For behavioral experiments, t-test was used to analyze SPT, DLT, OFT, FST and OF in Ant-34a-treated and Negative control mice. A two-way ANOVA (factor ANOVA) was used to compare the percentage of time spent in SIT (social and object stimulus) and NORT (object or old objects). For the analysis during the acquisition day of FCT, a two-way ANOVA was conducted. The factors considered were "Treatment" (with Ant-34a and Neg.Ctrl as levels) and "Time" (with Baseline, Stimulus 1, and Stimulus 2 as levels). The analyzed data concerning the duration in seconds of freezing behavior. For the analysis during the extinction phase of FCT, a similar two-way ANOVA was conducted. The factors were "Treatment" (with Ant-34a and Neg.Ctrl as levels) and Time (Day 1, Day 2, Day 3, and Day 4). The analyzed data focused on the duration in seconds of freezing behavior. A two-way ANOVA was used to compare the difference in velocity (cm/s) in LVT (free exploration and stimuli presentation) between Neg.Ctrl and Ant-34a groups. A one-way ANOVA was conducted to evaluate the differences in miR-34a expression levels across different genotypes. The genotype factor consisted of three groups: miR-34a$^{loxP/loxP}$, Gad2::Cre, and Gad2:C/miR-34$^{loxP/loxP}$. The analysis encompassed multiple tissues, including organs, plasma, and various brain structures. In all cases, a Fisher LSD was used for post-hoc analysis. All data were analyzed with Graphpad Prism v.8.

4. Results

4.1 miR-34a is Selectively Expressed in GABAergic Neurons in the DRN

DRN is known to exhibit notable miR-34a expression (Andolina et al., 2018; Lo Iacono et al., 2020). To further delve into the intricacies of miR-34a within this neural region, our current investigation adopts a multifaceted approach. Firstly, we leverage RNA scope technology coupled with immunofluorescence. This method allows us to meticulously scrutinize the precise localization of miR-34a within the ventrolateral region of the DRN. The use of immunofluorescence aids in identifying specific neuron types expressing miR-34a. In parallel, we employ a comprehensive genetic strategy involving in situ hybridization (ISH) analysis. This genetic approach is crucial for achieving a more profound understanding of cell-type miR-34a expression within the DRN. By utilizing various transgenic mouse lines, such as Gad2::Cre, miR-34$^{loxP/loxP}$, and GAD2/MiR-34$^{loxP/loxP}$, we aim to selectively delete miR-34a expression within GABAergic neurons. The integration of these two methodologies is strategic. RNA scope with immunofluorescence allows for a detailed examination at the cellular level, providing insights into the specific neuron types expressing miR-34a. On the other hand, the genetic strategy with ISH analysis offers a broader understanding of miR-34a's expression within the DRN by selectively modifying its expression.

4.1.1 Cellular strategy

Using a combined approach involving RNA scope technology and immunofluorescence methods, we established the selective localization of miR-34a within the ventrolateral region of the DRN. Our analysis provided evidence that miR-34a is found exclusively in GAD67-positive neurons, while evidently lacking presence in 5-HT-positive neurons. Importantly, this distinction had statistical significance ($t = 31.33$; $df = 5$; $p=0.0001$), as illustrated in Figures 1A and B.

Furthermore, we reported that approximately 67% of GAD67+ cells within the DRN showed expression of miR-34a whereas the remaining 33% did not (Figure

1C). This interesting observation suggests that miR-34a is selectively expressed within a specific subset of GABAergic neurons.

Finally, to evaluate the specificity of miR-34a probe and exclude nonspecific binding, we performed RNA scope assays on brain sections of constitutive miR-34 family KO mice. There was no detectable signal for miR-34a within the DRN, as presented in Figure 1D demonstrating a specificity of this method to label miR-34a-positive neurons.

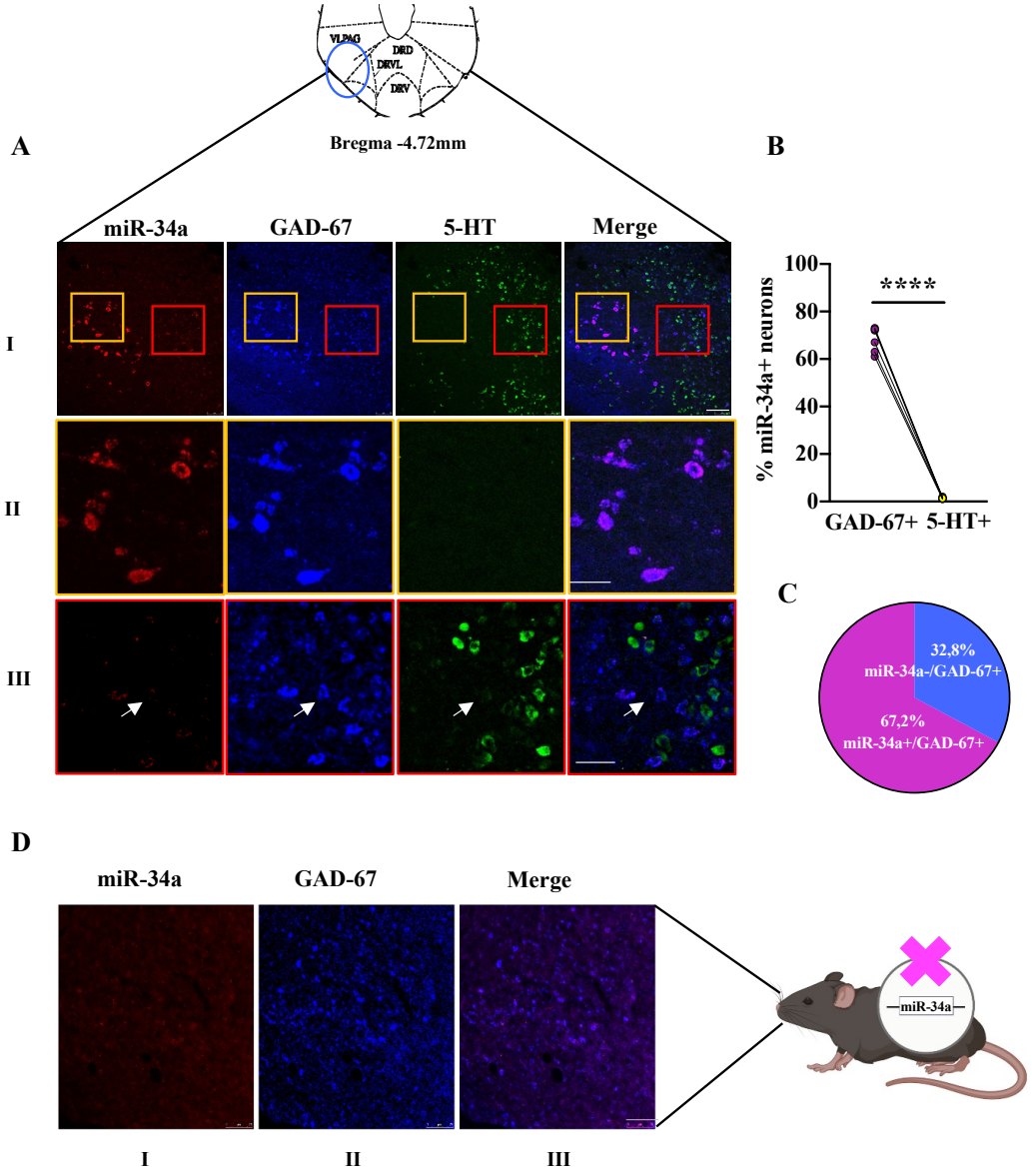

1. (A) Depicted are representative images of miRNAscope combined with immunofluorescence assays conducted on coronal brain sections at the level of the Dorsal Raphe Nucleus (DRN) region in C57BL/6 mice. The columns illustrate both low- and high-magnification views of a coronal brain section, while the rows

display triple-labeled confocal images of the DRN. These images show miR-34a (in red), serotonin (5-HT, in green), GAD67 (in blue), and the merged signals. In specific terms, (I) represents low-magnification images, (II) provides an example of GAD-67+/miR-34a+ colocalization, and (III) offers an example of GAD-67+/miR-34a colocalization. Scale bars for (I) low-magnification images are 100 μm, while those for (II) and (III) high-magnification images are 40 μm. (B) On the left panel, the percentage of miR-34a that colocalized with GAD-67 and 5-HT neurons in the DRN of C57BL/6 mice is presented (N = 3 per group, with 2 sections analyzed per animal). (C) A pie chart illustrates the percentage of GAD-67 cells expressing miR-34a. (D) Representative confocal images of miR-34a signal in TKO mice for miR- 34a, b,c on coronal section at the level of DRN. Labeled confocal images of miR-34a in red (I), GAD67 in green (II) and merged (III) signals showing the absence of miR-34a signal. Scale bar = 75 μm.

4.1.2 miR-34a expression in a mouse model carrying genetic deletion of miR-34a in GABAergic neurons

To further confirm the specific expression of miR-34a on GABAergic neurons within the DRN, we employed a genetic strategy combined with ISH analysis. This genetic approach involved the utilization of multiple transgenic mouse lines, including Gad2::Cre, miR-34$^{loxP/loxP}$, and Gad2::Cre/miR$^{34aloxP/loxP}$ mice, enabling precise targeting and visualization of miR-34a within the DRN.

Gad2::Cre mice allowed us to selectively knock down the miR-34a expression specifically within GABAergic neurons

To generate this animal model, we implemented a breeding strategy involving conditional knockout mice for miR-34 (miR-34$^{loxP/loxP}$) and mice carrying the CRE Recombinase gene under the control of a GABAergic promoter (Gad2::Cre). Successive generations of these mice were bred until achieving homozygous expression for both genes. Consequently, we established an animal model characterized by the specific genetic deletion of miR-34a's in GABAergic neurons, referred to as Gad2::Cre/miR$^{34aloxP/loxP}$ (Figure 2).

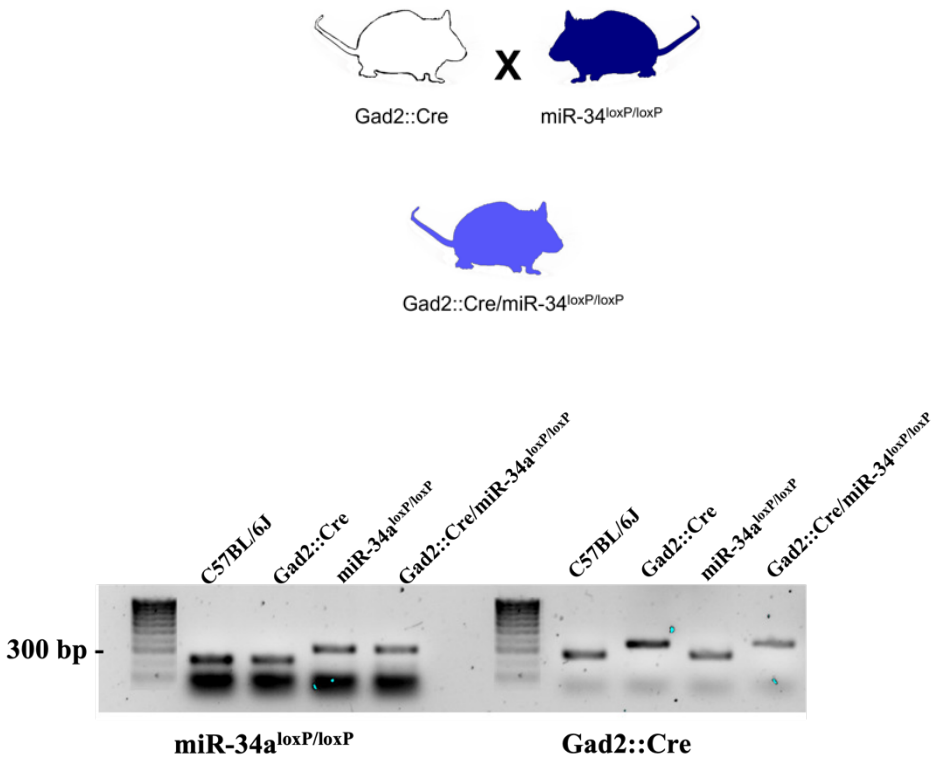

2. Schematic design of mice crossing was employed to generate the Gad2::Cre/miR$^{34aloxP/loxP}$ animal model. (B) Exemplificative PCR screening was conducted to confirm the presence of miR-34a floxed sites and the GAD67-dependent Cre site in the resulting mice.

Our analysis demonstrated a marked reduction in the number of miR-34a-positive cells in Gad2::Cre/miR-34$^{loxP/loxP}$ mice compared to WT, miR-34$^{loxP/loxP}$ and Gad2::Cre control groups (Figure 3A). Statistical analysis showed [F= 10.07; $p<0.0001$], a pronounced reduction in miR-34a-positive cells in Gad2::Cre/miR-34$^{loxP/loxP}$ mice ($p<0.0001$) compared to the other control groups.

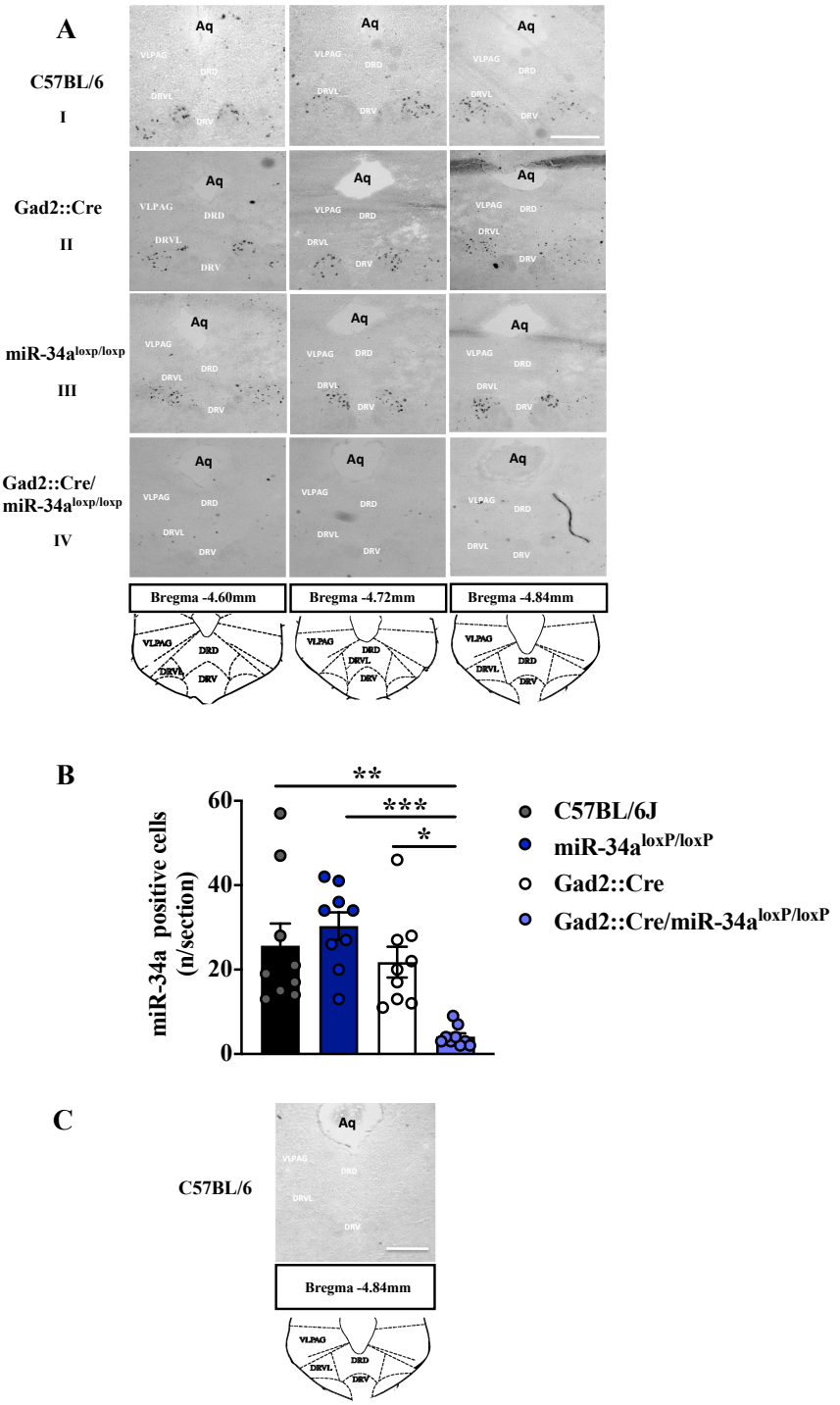

3. (A) Three representative coronal brain sections (along the rostro caudal axis) of C57BL/6 (I), Gad2::Cre (II), miR-34$^{loxP/loxP}$ (III), and Gad2::Cre/ miR-34$^{loxP/loxP}$ (IV) mice showing the miR-34a ISH signal in the DRN (Scale bar, 500 μm). (B) The mean ± SEM values for the number of miR-34a positive cells in the DRN were calculated across various experimental groups. Our analysis revealed a significant reduction in the number of miR-34a positive cells in Gad2::Cre/miR-34$^{loxP/loxP}$ mice when compared to C57BL/6, Gad2::Cre, and miR-34$^{loxP/loxP}$ mice (N = 3 animals per group, with 3 sections analyzed per animal). Statistical significance levels were denoted as follows: *P < 0.05, **P < 0.001, ***P < 0.0001. (C) In addition, no miR-34a signal was detected

in DRN coronal sections from C57BL6 mice when incubated with the scramble LNA probe (Scale bar = 500 μm).

These first set of results, we establish that within the DRN, miR-34a displays a distinguishable pattern of selective expression within a distinct subset of GABAergic neurons, as validated by the RNA scope technique.

4.2 Aversive and Rewarding Experiences Induce GABAergic Transmission Reduction in the DRN

Before to delving into the examination of miR-34a's role in DRN GABAergic neurotransmission, we assessed the DRN GABA release in response to to either an aversive or rewarding stimuli in C57BL/6 mice. The aversive and rewarding stimulus used are detailed in the Materials and Methods (pag 22; Section 3.6).

For the rewarding experience, we selected exposure to chocolate. This stimulus was chosen due to its capacity to evoke approaching and consummatory behavior in a standard feeding regime, as previously documented (Latagliata et al., 2018). Restraint stress served as the aversive condition, characterized by its severe and inescapable nature.

Two complementary experimental settings were employed, as depicted in Figures 4A and 4D. Firstly, by in-vivo microdialysis we measured extracellular GABA levels in the DRN during the two-hour exposure to respective stimuli. Secondly, by ex-vivo electrophysiology assessed miniature inhibitory postsynaptic currents (mIPSCs) on 5-HT neurons on acute slices of DRN from mice previously exposed to aversive or rewarding experiences.

Our results demonstrate that both restraint stress and white chocolate exposure significantly reduced GABA efflux in the DRN over time, as measured by in vivo microdialysis (main effect of time: $F(1, 14) = 6.352$, $p=0.0002$; Figure 4B). Specifically, in response to restraint stress, a marked decrease in extracellular GABA was observed at 60, 80, 100, and 120 minutes. Similarly, white chocolate exposure significantly reduced extracellular GABA efflux in the DRN (time points:

20 to 120 minutes from protocol onset, Figure 4B). Basal GABA levels remained stable over time in both experimental groups (stress: $p=0.41$; chocolate: $p=0.13$; Figure 4B), and no significant differences were found in baseline DRN GABA concentrations between the two groups ($t = 1.19$; $df = 14$; $p=0.253$, Figure 4C).

Confirming a decrease in presynaptic GABA release, exposure to both acute stress and white chocolate led to a reduction in the frequency, but not amplitude, of mIPSCs recorded from 5-HT neurons compared to the control group (no-stimulus) [(frequency: $F\ (2, 44) = 11.75$, $p<0.0001$; amplitude: $F\ (2, 44) = 1.45$, $p=0.14$; (Figure 4F and G)].

In vivo microdialysis and ex-vivo electrophysiology provided a comprehensive insight into modifications in GABAergic neurotransmission induced by these experiences, demonstrated that both aversive and rewarding experiences reduce GABAergic transmission in the DRN.

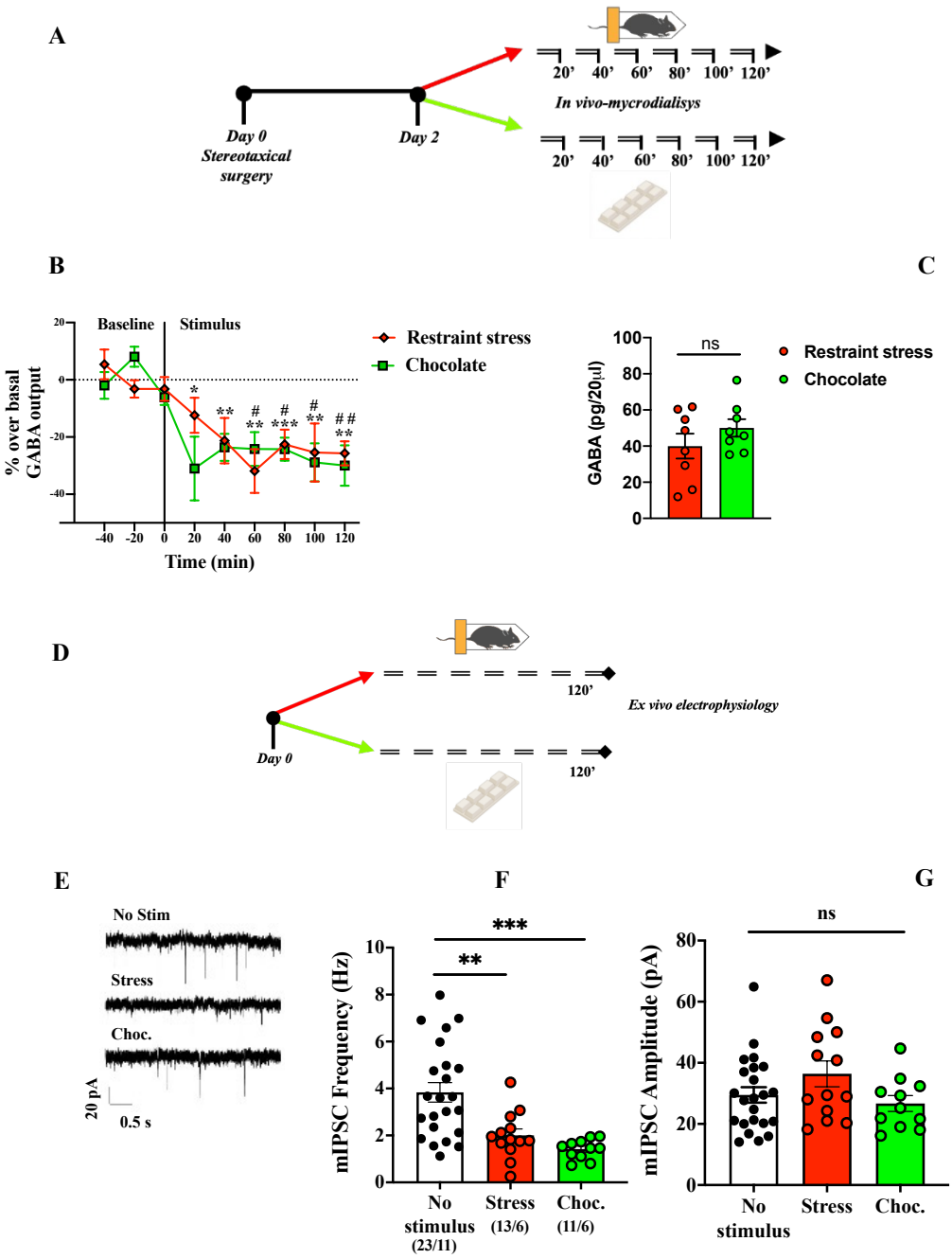

4. Exposure to aversive (restraint stress) or rewarding (white chocolate) stimuli results in a local reduction of GABA release within the DRN. The study utilized two main experimental techniques to assess GABA release in the DRN: in vivo microdialysis and ex vivo electrophysiology (timeline D). In In vivo microdialysis (timeline A), GABA release was monitored during the experiment, while ex vivo electrophysiology (timeline D) assessed GABA-related neuronal activity after a 120-minute exposure to restraint stress or white chocolate.

   The in vivo microdialysis findings presented in (B) demonstrate that both 120 minutes of restraint stress and white chocolate exposure caused a notable reduction in GABA levels within the DRN of C57BL/6 mice (restraint group N = 8; white chocolate group N = 8). Statistical significance was observed: *P < 0.05, **P < 0.01 from basal values (white chocolate group); #P < 0.05, ##P < 0.01 from basal

values (restraint stress group). Results are expressed as percentage changes (mean ± SEM) from basal values.
Moving to the electrophysiology section, the lower panel displays voltage-clamp spontaneous recordings (in DNQX+TTX) from DRN 5-HT neurons. Representative traces were captured in mice exposed to no stimulus, 2 hours of restraint stress, or 2 hours of white chocolate exposure (E). The right panels (F, G) show that the frequency, but not the amplitude, of miniature inhibitory post-synaptic currents (mIPSCs, mean ± SEM) was significantly lower in mice exposed to stress or chocolate compared to no stimulus (*P < 0.05, **P < 0.01, ***P < 0.001, ns: non-significant). The number of cells per number of animals (n/N) is indicated beneath each group in the panel associated with mIPSC frequency.

4.3 miR-34a Regulates DRN GABA Activity in Response to an Aversive, but Not a Rewarding Experience

Based on our previous findings regarding miR-34a expression in DRN GABAergic neurons, we aimed to ascertain its specific functional role in modulating GABA release in this region. We explored its regulatory function on GABA release in response to stimuli with different valences using a pharmacological approach to inhibit the miRNA's functionality. Specific inhibition of miR-34a in the DRN was achieved through intra-DRN injection of antagomiR-34a (Ant-34a) in C57BL/6 mice. A substantial reduction in miR-34a levels within the DRN was detected 2 hours, 48 hours, and 7 days post-Ant-34a injection (10 µM, 0.5 µL), but not with a non-targeted scrambled sequence (negative control) (Figure 5A).

Mice were infused with Ant-34a or its negative control into the DRN concurrently with the stressful procedure (Figure 5D). Under these conditions, the reduction in GABA efflux induced by restraint stress was evident only in mice injected with the control and not in those injected with Ant-34a, indicating the involvement of miR-34a in the DRN's response to acute stress [main treatment effect AB ($F(1, 13) = 172.7$; $p<0.0001$)], with significant differences between the Ant-34a and negative control groups at 20, 40, 60, and 100 minutes (Figure 5F). No significant differences were found in the absence of differences in baseline conditions, where DRN GABA efflux remained stable over time [(Neg. Ctrl-assigned: $p=0.30$, Ant-34a-assigned: $p=0.62$; (Figure 5H)].

Surprisingly, intra-DRN injection of Ant-34a (performed 48 hours prior, Figure 5E) did not alter local GABA release in mice exposed to chocolate compared to subjects injected with the negative control. A significant reduction in GABA levels in the DRN was observed in mice exposed to chocolate irrespective of treatment [time factor: $F(1, 13) = 4.511$; $p=0.0044$]. Specifically, in Ant-34a-treated mice, GABA levels were significantly lower at 20, 40, 60, 80, and 100 minutes (Figure 5G), while in negative control-treated mice, significant differences from baseline were found at 20, 40, 100, and 120 minutes from the start of the experience. GABA release remained stable over time in the baseline condition (Neg. Ctrl.: $p = 0.88$; Choc. Ant-34a: $p=0.86$; Figure 5G), and baseline concentrations did not differ between Ant-34a and negative control-injected mice ($t = 1.114$; $df = 13$; $p=0.285$, Figure 5I).

GABAergic signaling, assessed through electrophysiology, conducted after the aversive or rewarding experiences, displayed a comparable trend (Figure 5M; N): statistical examination using a two-way ANOVA indicated a significant effect of stimulus [$F(2,79) = 6.858$, $p=0.002$] and treatment [$F(1,79) = 4.539$, $p=0.036$; interaction: $F(2,79) = 2.542$, $p=0.08$] on mIPSC frequency. Conversely, there were no significant effects observed on mIPSC amplitude. Further analysis indicated that exposure to chocolate lowered mIPSC frequency in both the Ant-34a and negative control groups. However, restraint stress resulted in a reduction in frequency solely in the negative control group, while the Ant-34a group showed no change. Finally, we assessed whether Ant-34a affected chocolate consumption or latency. Our assessment revealed no significant alterations in either latency [$F(3, 42) = 1.006$, $p=0.474$] or chocolate consumption [$F(3, 42) = 2.055$, $p=0.141$] (Figure 5B and C). This indicates no change in behavior linked to reward stimulus between the 2 groups.

In summary, our findings demonstrate, for the first time, a role of miR-34a in regulating GABAergic neurotransmitter activity in a context-dependent manner.

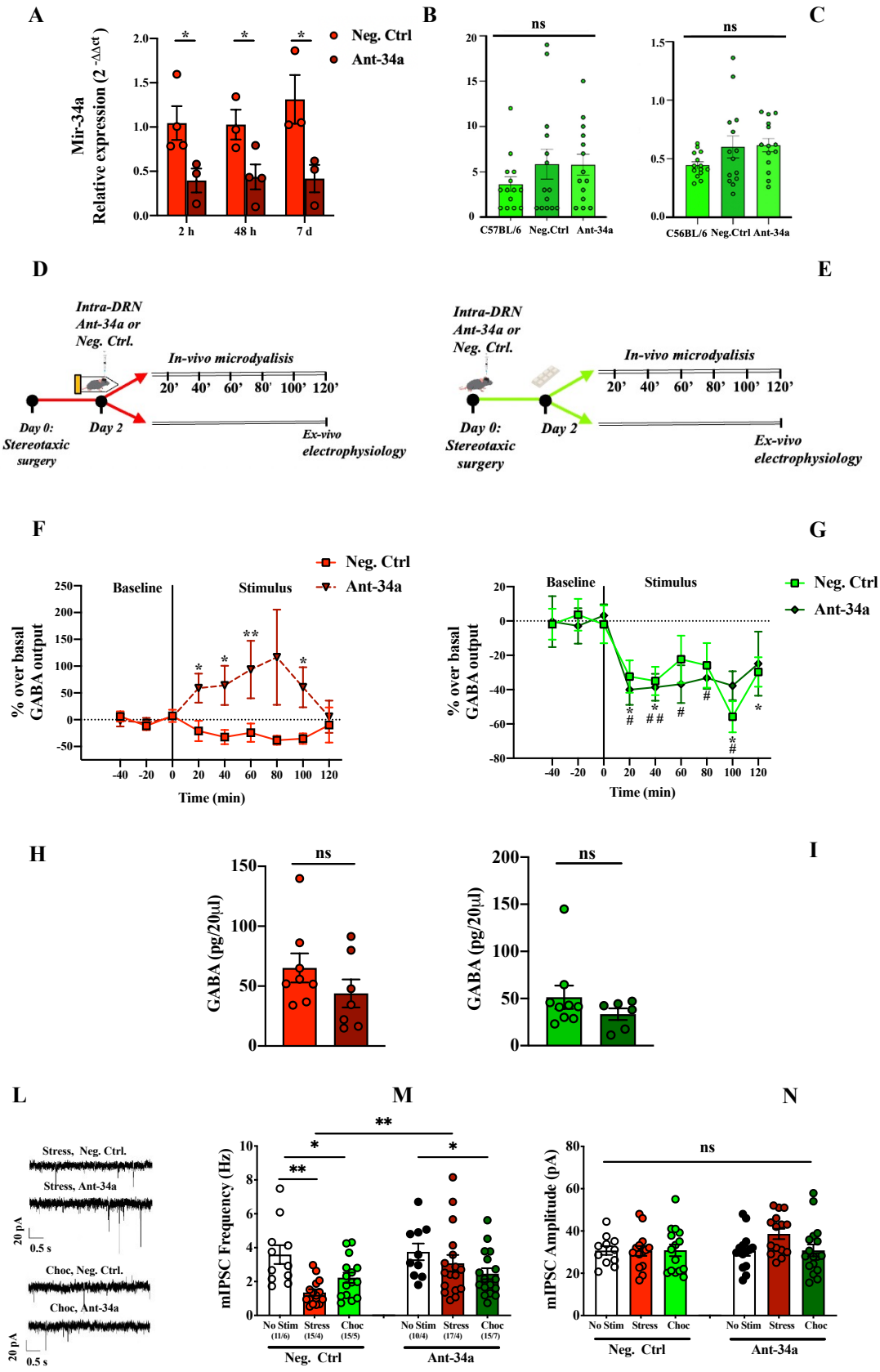

5. Ant-34a administration within the DRN resulted in a significant reduction of miR-34a levels, indicated by RT-qPCR measurements 2, 48, and 168 hours post intra-

DRN injection, compared to its negative control (Neg. Ctrl.) (*p < 0.05, Figure 5A). Infusion of Ant-34a in the DRN did not affect the approach or consumption behavior towards white chocolate in C57Bl/6 mice, as observed in the time taken to approach (B) and chocolate consumption (C) between groups that received Ant-34a or its Neg. Ctrl. (Figure 5B and 5C). Experimental timelines indicated the administration of Ant-34a or Neg. Ctrl. two days post stereotactic surgery. For stress protocols, the 2-hour stress relief procedure started immediately after Ant-34a administration (D). However, in the rewarding stimulus protocol, Ant-34a or Neg. Ctrl. was administered two days before exposure to white chocolate to prevent stress from immobilization (E). In vivo microdialysis revealed a time-dependent increase in GABA outflow following 120 minutes of restraint stress in C57BL/6 mice infused with Ant-34a (N = 7) compared to the Neg. Ctrl. group (N = 8) (*P < 0.05, Figure 5F). On the contrary, exposure to white chocolate significantly reduced GABA outflow irrespective of Ant-34a/Neg.Ctrl. treatment (Ant-34a group N = 6; Neg.Ctrl. group N = 9) (*P < 0.05, Figure 5G). (H; I) Baseline GABA levels in microdialysis experiments revealed no significant differences, indicated by 'ns.'(M) Representative mIPSC traces and (N) corresponding mean ± SEM of mIPSC frequency and amplitude recorded from 5-HT neurons showed significant changes post-stimulus or exposure compared to baseline values (*P < 0.05, **P < 0.01, ns: not significant). The cell count per animal (n/N) is provided in the respective panel.

4.4 GABAergic miR-34a in the DRN is Necessary for the Behavioral Response to Real Threat

Building on our electrophysiological and microdialysis results, which highlight the selective modulation of GABAergic neurotransmission by miR-34a in response to negative-valence stimulus, we aim to extend our exploration to the behavioral domain. We strategically chose a battery of behavioral tests, each well documented in the literature to be sensitive to DRN neurotransmission.

Given the role of miR-34a in preventing a decrease in GABA levels specifically during stressful stimuli and not rewarding stimuli such as white chocolate, we sought to investigate whether these specificities of miR-34a are reflected in context-specific behavioral responses. These include tests of memory for object (Lieben et al., 2006) and Fear Memory tests (Sengupta & Holmes, 2019a), recognized for their impact on cognitive function. Furthermore, we incorporate the social interaction and saccharin preference tests, to measure the behavioral response to positive valence stimuli. Finally, to assess to evaluate the behavioral responses in a negative valence context, we use the OFT (Nishitani et al., 2019) and the DLT (Johnson et

al., 2019), FST and the LVT(L. Huang et al., 2017). To evaluate the contribute of miR-34a in the DRN in governing these behavioral phenotypes, we performed intra-DRN ant-34a (and vehicle) infusion in WT mice.

Our results indicate that there were no significant differences observed between the two groups in the SIT (Figure 6B), where both presented a higher percentage of exploration for the conspecific rather than for the inanimate object [(F (1, 24) =92.07; p<0.0001)]. Furthermore, sucrose preference scores were insensitive to DRN Ant-34a infusion [(t = 1.032; df = 15; p=0.318, (Figure 6C)], suggesting a lack of impact on behaviors within the sucrose domain. positive valence, both in terms of reward and social interactions.

Importantly, in the cognitive domain, the three-day ORT showed no significant differences, indicating comparable memory for neutral stimuli [F (1,20) =26.82; p=0.0005; (Figure 6D)]. In the fear conditioning paradigm, there were no differences between the two groups in the acquisition of the conditioned stimulus implicated in treatment [F (1, 16) = 0.3686; p=0.5523 (Figure 6E)] or during the next four days of extinction, where only the conditioned stimulus (light) was present (Figure 6F).

Furthermore, in the negative valence domain, no differences were observed in the OFT nor in the distance moved [(t=0.4820; df=16; p=0.6364) (Figure 6G)] nor in the time spent at the center of the apparatus [(t=1.549; df=16; p=0.1410) (Figure 6H)] and infusion into the DRN did not change avoidance behavior in the DLT, as measured by time elapsed [(t=0.212; df=15; p= 0.834) (Figure 6I)] and the number of entries [(t=0.399; df=15; p=0.695) (Figure 6J)] in the light compartment, indicating a lack of impact on behaviors associated with anxiety and exposure to potential threats.

Interestingly, our analysis revealed that inhibition of miR-34a selectively alters behavioral responses specifically in the presence of real threatening stimuli. This impaired response is consistent with the lack of increase in immobility observed in the Forced Swim Test [(t = 4.511; df = 15; p= 0.0004) (Figure 6K)], an indicator of behavioral hopelessness. The Ant-34a group showed a significant lack of speed

increase compared to the Neg. Ctrl Group during the Looming stimulus presentation, as confirmed by statistical analysis [(F (1, 16) = 27.03; p<0.0001; (Figure 6L)]. These results highlight the selective involvement of miR-34a in the coding of real negative valence stimuli.

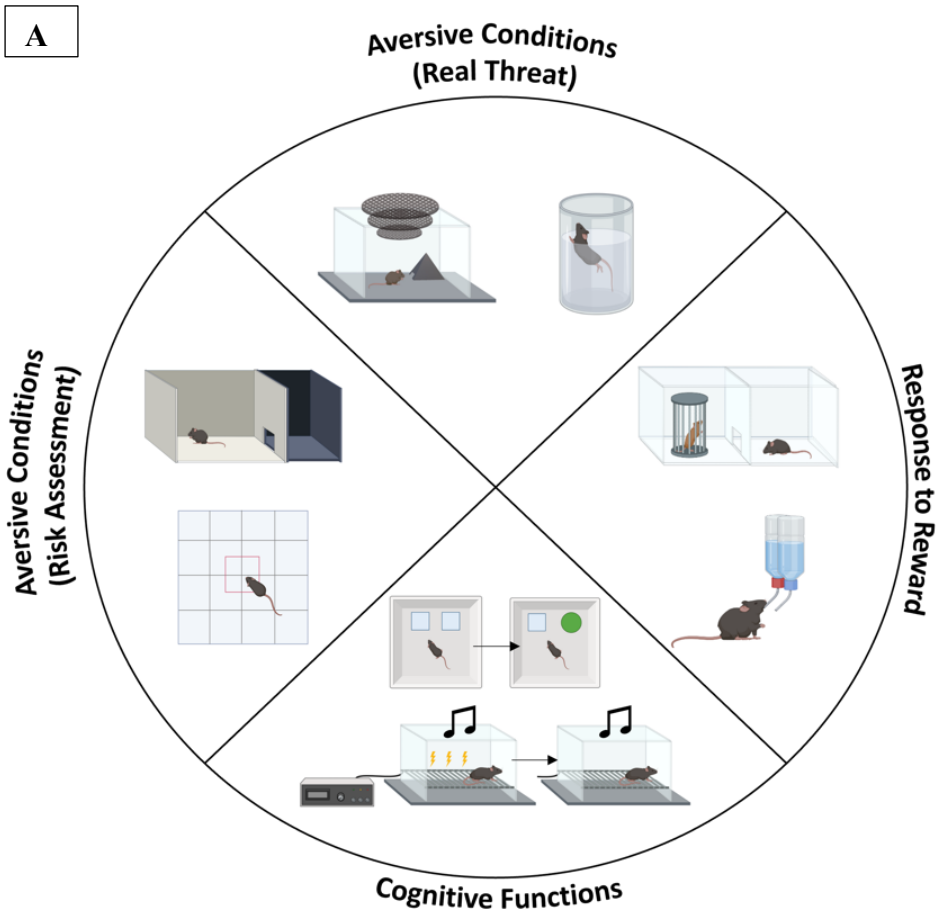

6. Diagram illustrating the contexts of behavioral tests conducted on mice, including the SIT and SPT for positive valence, the Novel Object NORT and FCT for cognitive domain, the OFT and DLT for negative valence risk assessment, the FST and LVT for aversive conditioning (real threat). Graphs on the next pages will show assessments: positive valence in green, cognitive domain in yellow, valence risk in pink, and aversive conditioning in red.

B

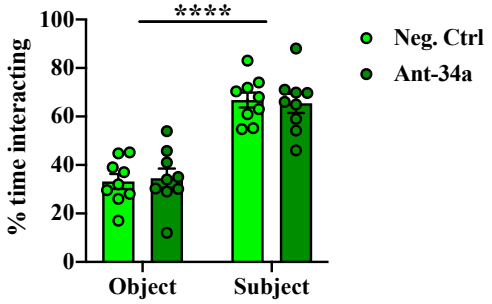
****
% time interacting
100
80
60
40
20
0
Object
Subject
Neg. Ctrl
Ant-34a

C

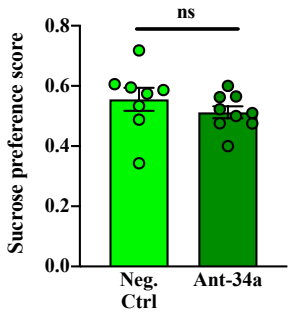
ns
Sucrose preference score
0.8
0.6
0.4
0.2
0.0
Neg. Ctrl
Ant-34a

D

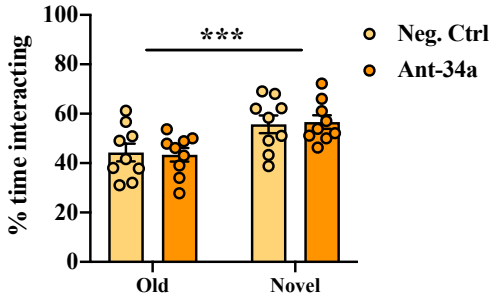
***
% time interacting
100
80
60
40
20
0
Old
Novel
Neg. Ctrl
Ant-34a

E

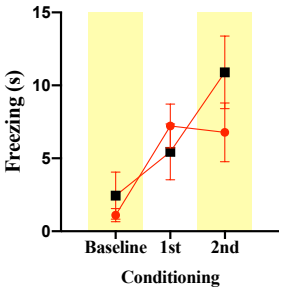
Freezing (s)
15
10
5
0
Baseline
1st
2nd
Conditioning

F

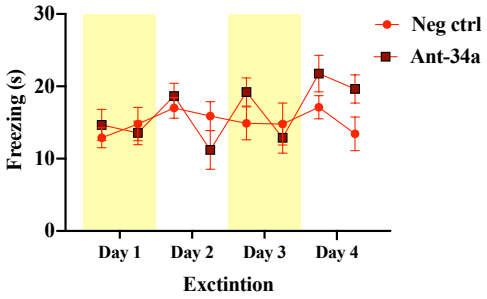
Freezing (s)
30
20
10
0
Day 1
Day 2
Day 3
Day 4
Exctintion
Neg ctrl
Ant-34a

G

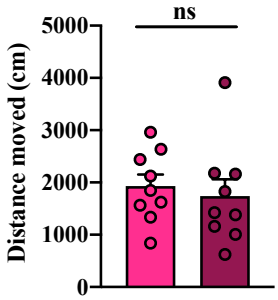
ns
Distance moved (cm)
5000
4000
3000
2000
1000
0

H

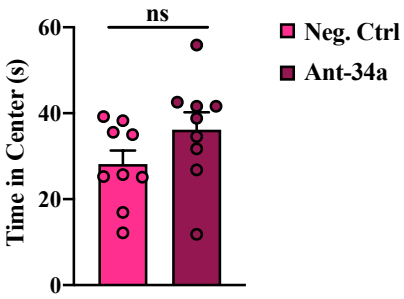
ns
Time in Center (s)
60
40
20
0
Neg. Ctrl
Ant-34a

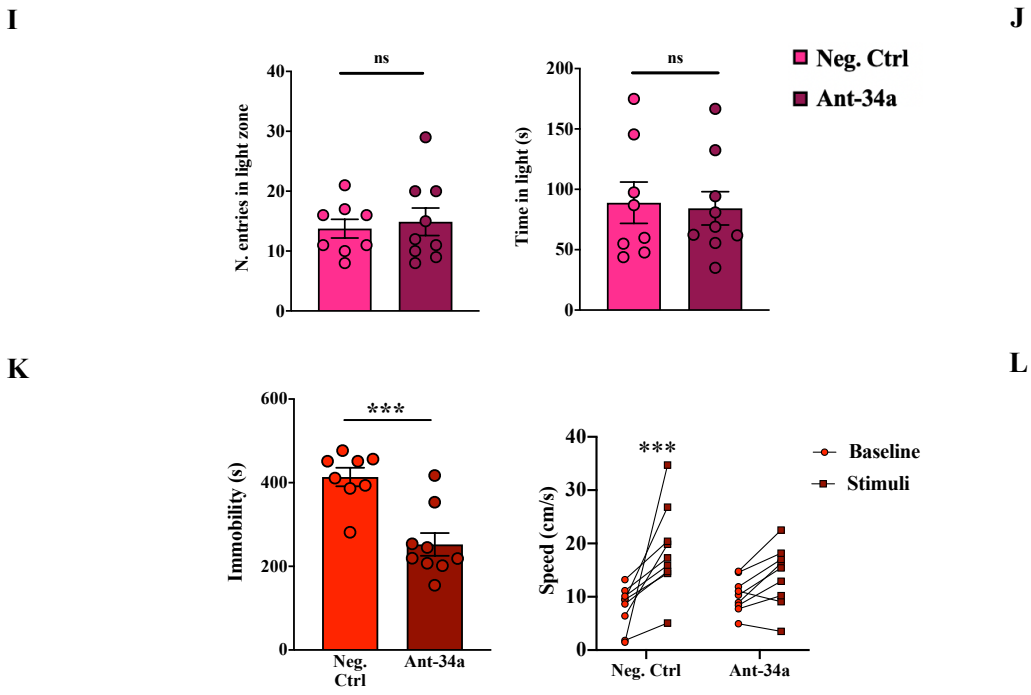

6. Effects of miR-34a inhibition in the DRN on various behavioral tests. Ant-34a or Neg. Ctrl was administered 2 days before the commencement of the tests. (B) Does not alter social interaction with the conspecific in the SIT. (C) Does not affect sucrose preference in the SPT. (D) Does not influence time spent with the novel object in the NORT. (E-F) Does not impact both the acquisition and extinction of conditioned stimulus in the FCT. (G-H) Does not modify locomotor activity or time spent in the center in the OFT. (I-J) Does not change both the time spent and the number of entries in the light compartment of the DLT. (K) While the inhibition significantly reduces immobility time in the FST. (L) The inhibition of miR-34a prevents the increase in speed during LVS. *P < 0.05, **P < 0.01, ***P < 0.001, ns: nonsignificant.

4.5 The miR-34a levels in GABAergic neurons of the DRN mirror miR-34a plasma levels

It has been demonstrated that changes in cimiRNAs may correlate with changes in brain tissue miRNA levels (Cogswell et al., 2008). Building upon this knowledge, our study aims to elucidate whether miR-34a expression in GABAergic neurons of the DRN is related with those observed at plasmatic level.

For this purpose, we employed qPCR to assess miR-34a expression in miR-34a$^{loxP/loxP}$, Gad2::Cre, and Gad2::Cre/miR-34a$^{loxP/loxP}$ animals, focusing our investigation on brain regions where high density of GABAergic neurons are

present, such as the medial Prefrontal Cortex (mPFC), Nucleus Accumbens (Nac), Hippocampus (Hipp), Central Amygdala (Cea), and DRN.

One-way ANOVA showed a significant effect of genotype on miR-34a level in the DRN [(F (2, 14) = 4.02; p=0.0417); (Figure 7F)]. Post-hoc analysis reported a significant difference in miR-34a level in the DRN between miR-34a$^{loxP/loxP}$ and Gad2::Cre/miR-34a$^{loxP/loxP}$ (p=0.0160), and a difference close to significant between Gad2::Cre and Gad2::Cre/miR-34a$^{loxP/loxP}$ (p=0.0546).

However, no significant differences in miR-34a expression were detected within the three groups in the mPFC [(F (2, 17) = 1.633; p=0.2246); (Figure 7B)], Nac [F (2, 18) = 0.9429; p=0.4079); (Figure 7C)], Hipp [(F (2, 16) = 0.1805; p=0.8366); (Figure 7D)], and Cea [(F (2, 20) = 1.133; p=0.3418); (Figure 7E)].

Additionally, we aimed to determine whether the observed miR-34a levels in GABAergic neurons of the DRN were related with those present in the plasma. Surprisingly, we found that miR-34a levels significantly decreased only in the Gad2::Cre/miR-34a$^{loxP/loxP}$ group [(F (2, 17) = 9.400; p=0.0018); (Figure 7G)] compared to control groups.

To determine if plasma miR-34a levels are indicative of those originating from the DRN rather than other organs, we examined several organs expressing high levels of miR-34a (Concepcion et al., 2012) (Figure 7A) and that might contribute to the plasma levels of micRNAs. These organs could potentially contribute to plasma microRNA levels through the active or passive release of extracellular vesicles containing miRNAs or through the secretion of miRNAs bound to proteins or in complexes with lipids that circulate in the plasma (Cui & Cui, 2020). We found no differences within groups in the thymus [F (2, 12) = 0.5012; p=0.6179); (Figure 7H)], heart [F (2, 8) = 0.7508; p=0.5025); (Figure 7I)], kidneys [F (2, 13) = 0.5080; p=0.6131); (Figure 7J)], lungs [F (2, 13) = 1.600; p=0.2122); (Figure 7K)], spleen [(F (2, 17) = 2.023; p=0.1629); (Figure 7L)], and testes [(F (2, 9) = 0.08174; p=0.9222); (Figure 7M)].

These findings suggest GABAergic neurons in the brain and more specifically in the DRN can represent one of the "sources “of circulating miR-34a.

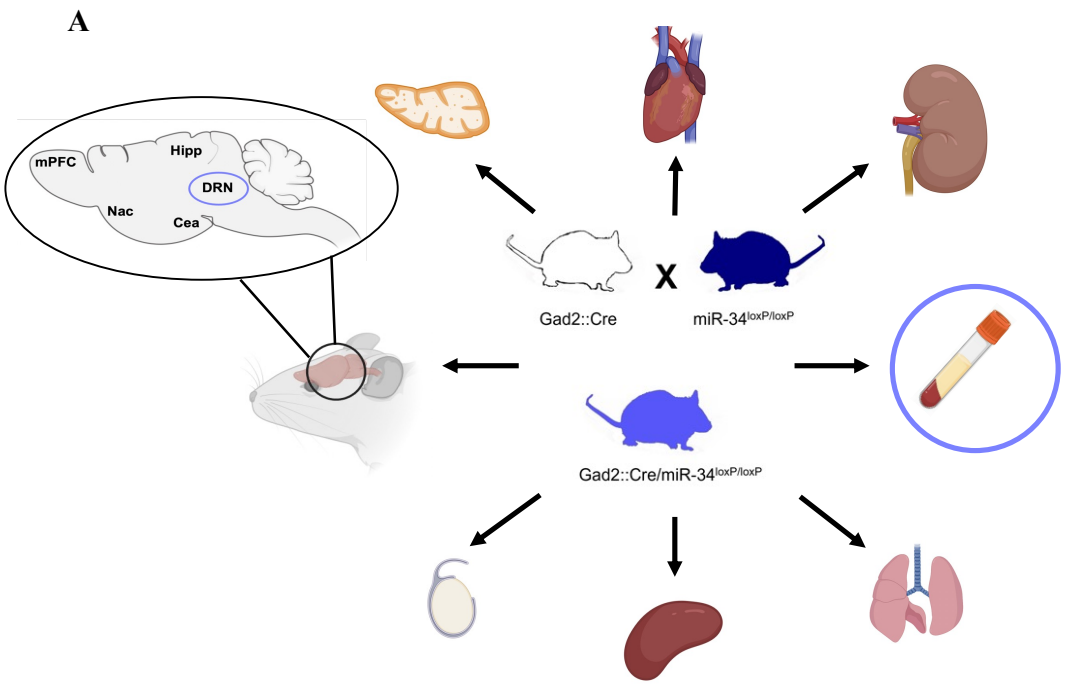

Gad2::Cre

MiR-34a$^{loxP/loxP}$

Gad2::Cre/miR-34a$^{loxP/loxP}$

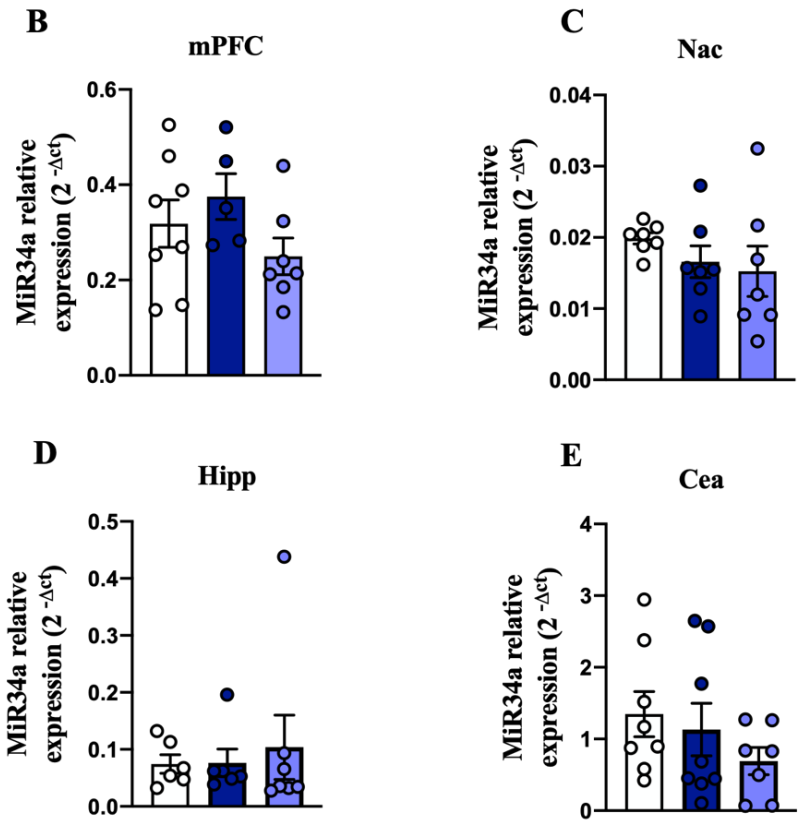

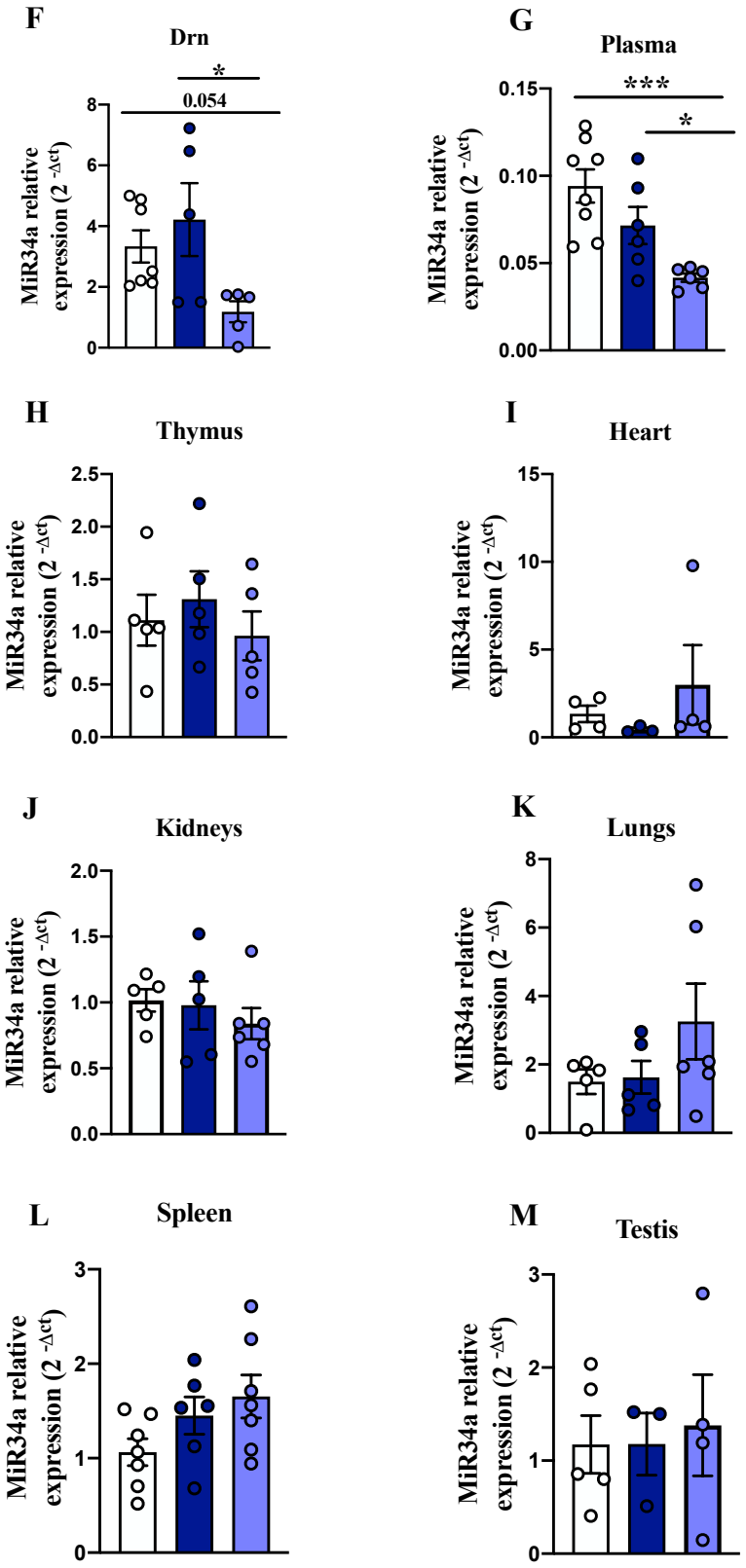
F
Drn
*
0.054
MiR34a relative expression (2 -Δct)
G
Plasma
***
*
H
Thymus
I
Heart
J
Kidneys
K
Lungs
L
Spleen
M
Testis

7. Genetic constitutive deletion of miR-34a specifically in GABAergic neurons (Gad2::Cre/miR-34a$^{loxP/loxP}$) leads to a pronounced reduction in miR-34a levels in the DRN (F) and plasma (G). It does not alter miR-34a levels in the mPFC (B), Nac (C), Hipp (D), thymus (H), heart (I), kidneys (J), lungs (K), spleen (L), and testes (M). *P < 0.05, **P < 0.01, ***P < 0.001.

4.6 Pharmacological inhibition of miR-34a in the DRN reduces Plasma miR-34a Levels

Building upon the observed decreased in miR-34a levels in both the DRN and plasma of genetically modified animals, we aimed to elucidate the influence of miR-34a expression specifically within the DRN on plasma miR-34a levels. To address this, we performed pharmacological inhibition of miR-34a directly into the DRN and subsequently we assessed the effects of this manipulation on plasma miR-34a levels in C57BL/6 mice (timeline 8A).

We observed decreased levels of miR-34a both in the DRN [(t=3.928, df=10, p= 0.0028); (Figure 8B)] and in plasma [(t=3.615, df=11, p=0.0041); (Figure 8C)] in subjects infused with Ant-34a compared to animals infused with the control sequence.

These findings suggest that GABAergic neurons of the DRN provide a source of plasma miR-34a levels.

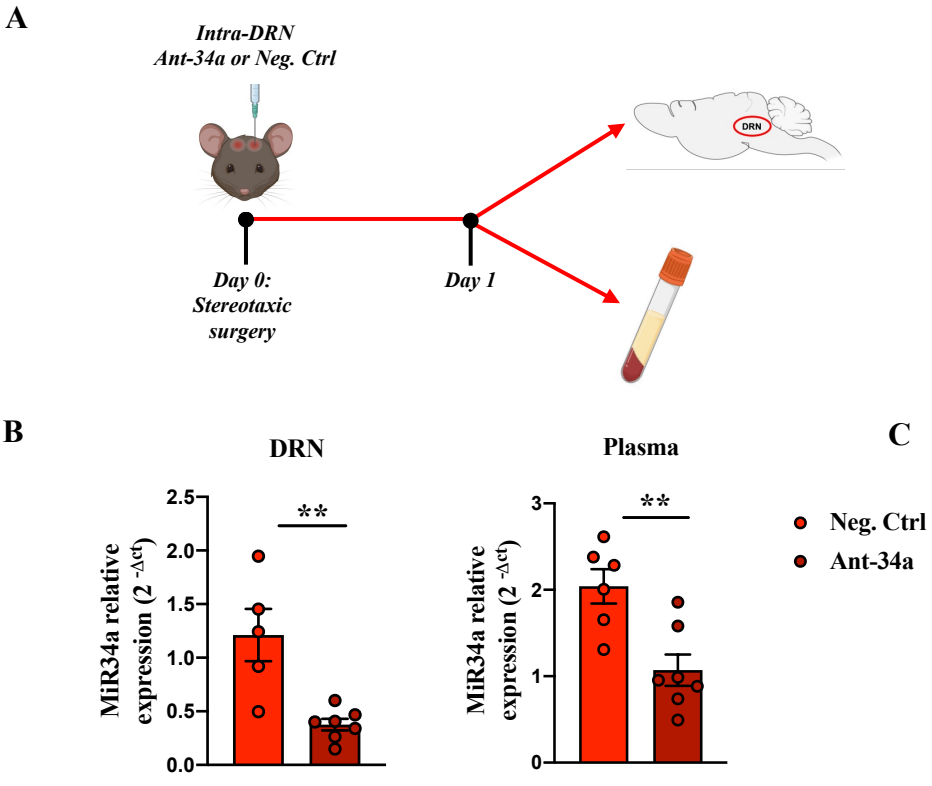

8. Inhibition of miR-34a in the DRN reduces miR-34a levels in plasma. Experimental timeline: Ant-34a or Neg. Ctrl were administered 1 day prior to the experiment. Intra-DRN infusion of Ant-34a altered miR-34a levels in the DRN (B) and plasma (C). *P < 0.05, **P < 0.01.

5. Discussion

In this study, we present several innovative findings. Specifically, we demonstrated that a) miR-34a is selectively expressed in a subpopulation of GABAergic neurons in the DRVL; b) miR-34a modulates GABAergic transmission in the DRN in a valence-dependent manner c) miR-34a influences behavioral response only in the presence of threatening stimuli; d) plasma miR-34a levels reflect miR-34a expression levels in GABAergic neurons of DRN.

The brain's ability to determine whether a stimulus is perceived as good or bad, known as emotional valence, is a crucial process for survival and well-being. Stimuli with specific valence is encoded by neural mechanisms that are highly context-dependent and undergo short- and long-term changes influenced by synaptic plasticity, and homeostatic demands (Tye, 2018).

Recent research has begun to investigate the neural substrates underlying the processing of specific emotional valence and how these circuits can be identified and modulated by specific molecules.

MicroRNAs have significant regulatory functions in organisms by targeting specific messenger RNAs (mRNAs) for cleavage or translational repression (Samynathan et al., 2023).
In recent years, it has been demonstrated that various miRNAs exhibit specific expression patterns in various cell types (He et al., 2012). Here, we have shown that miR-34a has emerged as a molecule with a specific distribution within the brain, particularly within a subset of GABAergic interneurons in the DR nucleus. The DRN neurons receive GABAergic inputs from both local interneurons and distal GABAergic cells originating from other brain structures (Hernández-Vázquez et al., 2019). The results from miRNAscope and ISH investigation revealed that the miR-34a signal is localized within soma-like structures, (Crawford et al., 2010; Matthiesen et al., 2017; Spoida et al., 2014) strongly indicating that miR-34a is expressed in local GABAergic neurons within the DRVL region. All these findings These findings align with another study on miRNA profiles in the mouse brain, which indicates that the miR-34 family, particularly the a and c isoforms, are

expressed in GABAergic neurons of the cerebellum during embryonic stages (He et al., 2012).

Our results also shed light on the heterogeneity of GABAergic neurons in this region. However, not all GABAergic neurons in the DRN show colocalization with the miR-34a signal. This observation is noteworthy considering the heterogeneity of inhibitory interneurons in the DRN, which are morphologically, electrically, and chemically diverse(Calizo et al., 2011; Hernández-Vázquez et al., 2019). A recent single-cell transcriptome study in mice identified at least three distinct GABAergic neuronal subtypes in this region(K. W. Huang et al., 2019). Future investigations will be crucial to clarify whether miR-34a is expressed in a specific subpopulation of DRN GABAergic cells.

Animals' studies have shown that GABAergic transmission of the DRN mediates responses to aversive and rewarding stimuli (Y. Li et al., 2016; Seo et al., 2019; Spoida et al., 2014). In response to a rewarding stimulus, both active (approach/consume) and passive (waiting) responses are associated with the inhibition of DRN GABAergic neurons (Seo et al., 2019). Conversely, in adverse experiences, active (escape or avoid) and passive (immobility) behavioral responses are associated with an increase and decrease in GABA activity, respectively(Seo et al., 2019).
In line with these findings, our in vivo microdialysis results revealed a decrease of GABA release in the DRN of WT mice exposed to a rewarding stimulus or a severe and unavoidable stressor where active coping is not allowed. Consistently, in ex vivo electrophysiology experiments, we demonstrated that of mIPSC frequency recorded from 5-HT neurons decreased during both stimuli. This finding confirms GABAergic transmission as a key cell population in the regulation of 5-HT neurons in the DRN (Challis et al., 2013) in response to positive and negative valence stimuli.

Interestingly, we found that miR-34a inhibition modifies the DRN GABA release and mIPSC frequency on 5-HT neurons of mice subjected to the stressor, but not in response to exposure to palatable food, highlighting a specific regulatory function of locally expressed miR-34a in modulating GABAergic transmission within the

DRN. The regulation of neurotransmission by miR-34a aligns with previous findings indicating its involvement in the acute modulation of synaptic transmission (Berentsen et al., 2020). Furthermore, several mRNAs encoding proteins that regulate neurotransmitter release in the DRN are confirmed targets of miR-34a, including 5-HT2C (Lo Iacono et al., 2021), CRFR1 (Dias et al., 2014; Haramati et al., 2011), and synaptotagmin-1 (Agostini, Tucci, Killick, et al., 2011).

The function of specific neural circuits supports specific behavioral strategies necessary for survival and adaptation to environmental challenges (Devineni & Scaplen, 2022). The neurotransmission in the DRN is involved in a wide range of behaviors, including risk assessment, defensive reactions towards a threat, social behavior, reward seeking (Paquelet et al., 2022; J. Ren et al., 2018; Sengupta & Holmes, 2019).

The FST and LVT represents a negative experience in which the animal is faced with a real threat eliciting an immediate and innate defensive response in mice and that which impose unavoidable exposure to the threatening stimuli (Commons et al., 2017; De Franceschi et al., 2016). The DLT and open field test represent a negative valence stimulus linked to risk -assessment. Infact, in these tests animals can easily avoid the aversive conditions by refraining from entering the illuminated or open space. We found that pharmacological inhibition of miR-34a in the DRN had no impact on avoidance of the aversive compartment in the DLT or on the time spent in the center of the open field. Instead, this manipulation reduced the expression of passive defensive responses (immobility) in mice exposed to the FST and impairs escaping behavior in response to the threat visual stimuli in the LVT. In the FST immobility behavior represent an adaptive coping response to an aversive and inescapable situation. Instead, it prevents a beneficial expenditure of energy, thereby impeding the ability to capitalize on unforeseeable opportunities to escape the situation (Cabib & Puglisi-Allegra, 2012; De Kloet & Molendijk, 2016). Similarly, the absence of escaping attempts in response to looming visual stimuli suggests a disruption in the typical defensive behavioral response. It is noteworthy that inhibition of miR-34a in the DRN did not modify the performance to the FCT and ORT, demonstrating that this manipulation did not alter the cognitive sphere.

Finally, miR-34a inhibition didn't affect the behavior associated with positive valence stimuli, such as chocolate consumption, SPT, and SIT, remained unaffected. These behavioral experiments demonstrated that miR-34a in the DRN play a role selectively in behavioral defensive response in the presence of a threat.

Depending on the context, the DRN provides 5-HT to a subset of brain regions (Hornung, 2003), and this activity is finely controlled by local GABAergic circuits (Boothman et al., 2006). For instance, 5-HT neurons expressing the vesicular glutamate transporter 3 are in the median areas of the DRN, projecting primarily to regions such as the VTA and are implicated in the regulation and encoding of positive valence stimuli (reward)(Luo et al., 2015; H. L. Wang et al., 2019). Meanwhile, it has been demonstrated that DRN-mpFC connections are involved in encoding negative valence stimuli such as stress (Amat et al., 2005; Andolina et al., 2018; Ren et al., 2018; Waselus et al., 2011).
Consequently, distinct subpopulations of GABAergic cells may be activated by different stimuli, subsequently influencing different 5-HT neurons targeting specific response areas. Supporting this notion, recent studies have identified discrete subsets of GABAergic cells encoding specific stimuli in the mPFC and the Cea(Cummings et al., 2022; Yang et al., 2023). Furthermore, previous reports have demonstrated that both constitutive and conditional deletion of miR-34a in mice attenuates severe stress-induced 5-HT release in the mPFC (Andolina et al., 2016; Lo Iacono et al., 2020). In this context, our data suggest that miR-34a expressed in the DRN may modulate GABAergic activity on specific subsets of local 5-HT neurons, potentially facilitating 5-HT release in selected target structures. It would therefore be of interest to investigate whether miR-34a-expressing GABAergic neurons establish synaptic connections with a subpopulation of 5-HT neurons projecting to either one or a subset of target area.

Ultimately, our findings have demonstrated a role of miR-34a in modulating adaptive behavioral responses to real threatening stimuli and support the conclusion that this molecule may identify a circuit within the DRN selectively engaged in the behavioral response to specific environmental challenges.

MiRNAs can be easily detected in both human and animal plasma and are promising for future clinical applications due to their stability in body fluids (Lan et al., 2015; Schwarzenbach et al., 2014). Growing evidences report that the circulating miRNAs could are modulated by for mental disease such as anxiety and depression and stress (Honda et al., 2013; Maffioletti et al., 2014).

Thus, from a translational perspective, our studies investigated the association between miR-34a levels in the CNS and periphery.
We found a selective reduction of plasma miR-34a levels in mice carrying genetic deletion of this molecule in GABAergic neurons as well as in those who received pharmacological inhibition miR-34a in the DRN. These data strongly support the existence of a relationship between plasmatic miR-34a and GABAergic miR-34a in the DRN. More specifically, these findings suggest that plasmatic miR-34a originate from the brain, and specifically from the DRN.
The potential for DRN GABAergic neurons to serve as a source of plasma miR-34a, offering prospects for detecting dynamic variations in miR-34a expression in the DRN in the bloodstream. These variations may likely mirror physiological or pathological responses to valence-specific stimuli.

In conclusion, these data show, for the first time, that miR-34a in the brain exhibits high specificity of expression and function. However, further experiments will be necessary to explore the possibility that other miRNAs in the Central Nervous System may demonstrate selective activity.
These findings significantly broaden our understanding of miRNA regulatory mechanisms, shedding light on their role as functional signatures of specific neuronal subpopulations with valence-specific functions.

From a therapeutic standpoint, the identification of the biological underpinnings of specific valence system behaviors, particularly in response to real and severe negative stimuli, represents a milestone in the development of novel treatments based on the pathophysiology of psychiatric disorders, advancing towards precision medicine for mental illnesses.

References

Abràmoff, M. D. (n.d.). *Image Processing with ImageJ*.

Agostini, M., Tucci, P., Killick, R., Candi, E., Sayan, B. S., Di Val Cervo, P. R., Nicoterad, P., McKeon, F., Knight, R. A., Mak, T. W., & Melino, G. (2011). Neuronal differentiation by TAp73 is mediated by microRNA-34a regulation of synaptic protein targets. *Proceedings of the National Academy of Sciences of the United States of America*, *108*(52), 21093–21098. https://doi.org/10.1073/pnas.1112061109

Agostini, M., Tucci, P., Steinert, J. R., Shalom-Feuerstein, R., Rouleau, M., Aberdam, D., Forsythe, I. D., Young, K. W., Ventura, A., Concepcion, C. P., Han, Y. C., Candi, E., Knight, R. A., Mak, T. W., & Melino, G. (2011). microRNA-34a regulates neurite outgrowth, spinal morphology, and function. *Proceedings of the National Academy of Sciences of the United States of America*, *108*(52), 21099–21104. https://doi.org/10.1073/pnas.1112063108

Amat, J., Baratta, M. V., Paul, E., Bland, S. T., Watkins, L. R., & Maier, S. F. (2005). Medial prefrontal cortex determines how stressor controllability affects behavior and dorsal raphe nucleus. *Nature Neuroscience*, *8*(3), 365–371. https://doi.org/10.1038/nn1399

Andolina, D., Di Segni, M., Accoto, A., Lo Iacono, L., Borreca, A., Ielpo, D., Berretta, N., Perlas, E., Puglisi-Allegra, S., & Ventura, R. (2018). MicroRNA-34 Contributes to the Stress-related Behavior and Affects 5-HT Prefrontal/GABA Amygdalar System through Regulation of Corticotropin-releasing Factor Receptor 1. *Molecular Neurobiology*, *55*(9), 7401–7412. https://doi.org/10.1007/s12035-018-0925-z

Andolina, D., Di Segni, M., Bisicchia, E., D'Alessandro, F., Cestari, V., Ventura, A., Concepcion, C., Puglisi-Allegra, S., & Ventura, R. (2016a). Effects of lack of microRNA-34 on the neural circuitry underlying the stress response and anxiety. *Neuropharmacology*, *107*, 305–316. https://doi.org/10.1016/j.neuropharm.2016.03.044

Andolina, D., Di Segni, M., Bisicchia, E., D'Alessandro, F., Cestari, V., Ventura, A., Concepcion, C., Puglisi-Allegra, S., & Ventura, R. (2016b). Effects of lack of microRNA-34 on the neural circuitry underlying the stress response and anxiety. *Neuropharmacology*, *107*, 305–316. https://doi.org/10.1016/j.neuropharm.2016.03.044

Andolina, D., Maran, D., Valzania, A., Conversi, D., & Puglisi-Allegra, S. (2013). Prefrontal/amygdalar system determines stress coping behavior through 5-HT/GABA connection. *Neuropsychopharmacology*, *38*(10), 2057–2067. https://doi.org/10.1038/npp.2013.107

Ashraf, S. I., McLoon, A. L., Sclarsic, S. M., & Kunes, S. (2006). Synaptic protein synthesis associated with memory is regulated by the RISC pathway in Drosophila. *Cell*, *124*(1), 191–205. https://doi.org/10.1016/j.cell.2005.12.017

Azevedo, J. A., Carter, B. S., Meng, F., Turner, D. L., Dai, M., Schatzberg, A. F., Barchas, J. D., Jones, E. G., Bunney, W. E., Myers, R. M., Akil, H., Watson, S. J., & Thompson, R. C. (2016). The microRNA network is altered in anterior cingulate cortex of patients with unipolar and bipolar depression. *Journal of Psychiatric Research*, *82*, 58–67. https://doi.org/10.1016/j.jpsychires.2016.07.012

Balakathiresan, N. S., Chandran, R., Bhomia, M., Jia, M., Li, H., & Maheshwari, R. K. (2014). Serum and amygdala microRNA signatures of posttraumatic stress: Fear correlation and biomarker potential. *Journal of Psychiatric Research*, *57*(1), 65–73. https://doi.org/10.1016/j.jpsychires.2014.05.020

Barbano, M. F., Wang, H. L., Zhang, S., Miranda-Barrientos, J., Estrin, D. J., Figueroa-González, A., Liu, B., Barker, D. J., & Morales, M. (2020). VTA Glutamatergic Neurons Mediate Innate Defensive Behaviors. *Neuron*, *107*(2), 368-382.e8. https://doi.org/10.1016/j.neuron.2020.04.024

Bartel, D. P. (2004). MicroRNAs: Genomics, Biogenesis, Mechanism, and Function. In *Cell* (Vol. 116, Issue 2, pp. 281–297). Cell Press. https://doi.org/10.1016/S0092-8674(04)00045-5

Beier, K. T., Steinberg, E. E., Deloach, K. E., Xie, S., Miyamichi, K., Schwarz, L., Gao, X. J., Kremer, E. J., Malenka, R. C., & Luo, L. (2015). Circuit Architecture of VTA Dopamine Neurons Revealed by Systematic Input-Output Mapping. *Cell*, *162*(3), 622–634. https://doi.org/10.1016/j.cell.2015.07.015

Beliveau, V., Svarer, C., Frokjaer, V. G., Knudsen, G. M., Greve, D. N., & Fisher, P. M. (2015). Functional connectivity of the dorsal and median raphe nuclei at rest. *NeuroImage*, *116*, 187–195. https://doi.org/10.1016/j.neuroimage.2015.04.065

Berentsen, B., Patil, S., Rønnestad, K., Goff, K. M., Pajak, M., Simpson, T. I., Wibrand, K., & Bramham, C. R. (2020). MicroRNA-34a Acutely Regulates Synaptic Efficacy in the Adult Dentate Gyrus In Vivo. *Molecular Neurobiology*, *57*(3), 1432–1445. https://doi.org/10.1007/s12035-019-01816-1

Beveridge, N. J., Gardiner, E., Carroll, A. P., Tooney, P. A., & Cairns, M. J. (2010). Schizophrenia is associated with an increase in cortical microRNA biogenesis. *Molecular Psychiatry*, *15*(12), 1176–1189. https://doi.org/10.1038/mp.2009.84

Bhattacharya, M., Sharma, A. R., Sharma, G., Patra, B. C., Nam, J. S., Chakraborty, C., & Lee, S. S. (2017). The crucial role and regulations of miRNAs in zebrafish development. In *Protoplasma* (Vol. 254, Issue 1, pp. 17–31). Springer-Verlag Wien. https://doi.org/10.1007/s00709-015-0931-1

Bicker, S., Khudayberdiev, S., Weiß, K., Zocher, K., Baumeister, S., & Schratt, G. (2013). The DEAH-box helicase DHX36 mediates dendritic localization of the neuronal precursor-microRNA-134. *Genes and Development*, *27*(9), 991–996. https://doi.org/10.1101/gad.211243.112

Bocchio-Chiavetto, L., Maffioletti, E., Bettinsoli, P., Giovannini, C., Bignotti, S., Tardito, D., Corrada, D., Milanesi, L., & Gennarelli, M. (2013). Blood microRNA changes in depressed patients during antidepressant treatment. *European Neuropsychopharmacology*, *23*(7), 602–611. https://doi.org/10.1016/j.euroneuro.2012.06.013

Boothman, L., Raley, J., Denk, F., Hirani, E., & Sharp, T. (2006). In vivo evidence that 5-HT 2C receptors inhibit 5-HT neuronal activity via a GABAergic mechanism. *British Journal of Pharmacology*, *149*(7), 861–869. https://doi.org/10.1038/sj.bjp.0706935

Cabib, S., & Puglisi-Allegra, S. (1991). Genotype-dependent effects of chronic stress on apomorphine-induced alterations of striatal and mesolimbic dopamine metabolism. *Brain Research*, *542*(1), 91–96. https://doi.org/10.1016/0006-8993(91)91002-I

Cabib, S., & Puglisi-Allegra, S. (2012). The mesoaccumbens dopamine in coping with stress. In *Neuroscience and Biobehavioral Reviews* (Vol. 36, Issue 1, pp. 79–89). https://doi.org/10.1016/j.neubiorev.2011.04.012

Calizo, L. H., Akanwa, A., Ma, X., Pan, Y. Z., Lemos, J. C., Craige, C., Heemstra, L. A., & Beck, S. G. (2011). Raphe serotonin neurons are not homogenous: Electrophysiological, morphological and neurochemical evidence. *Neuropharmacology*, *61*(3), 524–543. https://doi.org/10.1016/j.neuropharm.2011.04.008

Cardozo Pinto, D. F., Yang, H., Dorocic, I. P., De Jong, J. W., Han, V. J., Peck, J. R., Zhu, Y., Liu, C., Beier, K. T., Smidt, M. P., & Lammel, S. (2019). Characterization of transgenic mouse models targeting neuromodulatory systems reveals organizational principles of the dorsal raphe. In *Nature Communications* (Vol. 10).

Chakraborty, C., Sharma, A. R., Sharma, G., & Lee, S. S. (2021). Therapeutic advances of miRNAs: A preclinical and clinical update. In *Journal of Advanced Research* (Vol. 28, pp. 127–138). Elsevier B.V. https://doi.org/10.1016/j.jare.2020.08.012

Challis, C., Beck, S. G., & Berton, O. (2014). Optogenetic modulation of descending prefrontocortical inputs to the dorsal raphe bidirectionally bias socioaffective choices after social defeat. *Sec. Individual and Social Behaviors*, *8*. https://doi.org/10.3389/fn

Challis, C., Boulden, J., Veerakumar, A., Espallergues, J., Vassoler, F. M., Christopher Pierce, R., Beck, S. G., & Berton, O. (2013). Raphe GABAergic neurons mediate the acquisition of avoidance after social defeat. *Journal of Neuroscience*, *33*(35), 13978–13988. https://doi.org/10.1523/JNEUROSCI.2383-13.2013

Chandler, D. J., Lamperski, C. S., & Waterhouse, B. D. (2013). Identification and distribution of projections from monoaminergic and cholinergic nuclei to functionally differentiated subregions of prefrontal cortex. *Brain Research*, *1522*, 38–58. https://doi.org/10.1016/j.brainres.2013.04.057

Chen, J., & Condron, B. G. (2008). Branch architecture of the fly larval abdominal serotonergic neurons. *Developmental Biology*, *320*(1), 30–38. https://doi.org/10.1016/j.ydbio.2008.03.038

Chen, Y., An, Q., Yang, S. T., Chen, Y. L., Tong, L., & Ji, L. L. (2022). MicroRNA-124 attenuates PTSD-like behaviors and reduces the level of inflammatory cytokines by downregulating the expression of TRAF6 in the hippocampus of rats following single-prolonged stress. *Experimental Neurology*, *356*. https://doi.org/10.1016/j.expneurol.2022.114154

Cheng, C. Y., Hwang, C. Il, Corney, D. C., Flesken-Nikitin, A., Jiang, L., Öner, G. M., Munroe, R. J., Schimenti, J. C., Hermeking, H., & Nikitin, A. Y. (2014). MiR-34 Cooperates with p53 in Suppression of Prostate Cancer by Joint Regulation of Stem Cell Compartment. *Cell Reports*, *6*(6), 1000–1007. https://doi.org/10.1016/j.celrep.2014.02.023

Clarke, H. F., Dalley, J. W., Crofts, H. S., Robbins, T. W., & Roberts, A. C. (2004). Cognitive Inflexibility after Prefrontal Serotonin Depletion. *Science*, *304*(5672), 878–880. https://doi.org/10.1126/science.1094987

Cogswell, J. P., Ward, J., Taylor, I. A., Waters, M., Shi, Y., Cannon, B., Kelnar, K., Kemppainen, J., Brown, D., Chen, C., Prinjha, R. K., Richardson, J. C., Saunders, A. M., Roses, A. D., & Richards, C. A. (2008). Identification of miRNA changes in Alzheimer's disease brain and CSF yields putative

biomarkers and insights into disease pathways. *Journal of Alzheimer's Disease*, *14*(1), 27–41. https://doi.org/10.3233/JAD-2008-14103

Cohen, J. L., Ata, A. E., Jackson, N. L., Rahn, E. J., Ramaker, R. C., Cooper, S., Kerman, I. A., & Clinton, S. M. (2017). Differential stress induced c-Fos expression and identification of region-specific miRNA-mRNA networks in the dorsal raphe and amygdala of high-responder/low-responder rats. *Behavioural Brain Research*, *319*, 110–123. https://doi.org/10.1016/j.bbr.2016.11.015

Commons, K. G. (2020). Dorsal raphe organization. In *Journal of Chemical Neuroanatomy* (Vol. 110). Elsevier B.V. https://doi.org/10.1016/j.jchemneu.2020.101868

Commons, K. G., Cholanians, A. B., Babb, J. A., & Ehlinger, D. G. (2017). The Rodent Forced Swim Test Measures Stress-Coping Strategy, Not Depression-like Behavior. In *ACS Chemical Neuroscience* (Vol. 8, Issue 5, pp. 955–960). American Chemical Society. https://doi.org/10.1021/acschemneuro.7b00042

Concepcion, C. P., Han, Y. C., Mu, P., Bonetti, C., Yao, E., D'Andrea, A., Vidigal, J. A., Maughan, W. P., Ogrodowski, P., & Ventura, A. (2012). Intact p53-dependent responses in miR-34-deficient mice. *PLoS Genetics*, *8*(7). https://doi.org/10.1371/journal.pgen.1002797

Crawford, L. T. K., Craige, C. P., & Beck, S. G. (2010). Increased intrinsic excitability of lateral wing serotonin neurons of the dorsal raphe: A mechanism for selective activation in stress circuits. *Journal of Neurophysiology*, *103*(5), 2652–2663. https://doi.org/10.1152/jn.01132.2009

Cui, C., & Cui, Q. (2020). The relationship of human tissue microRNAs with those from body fluids. *Scientific Reports*, *10*(1). https://doi.org/10.1038/s41598-020-62534-6

Cummings, K. A., Bayshtok, S., Dong, T. N., Kenny, P. J., & Clem, R. L. (2022). Control of fear by discrete prefrontal GABAergic populations encoding valence-specific information. *Neuron*, *110*(18), 3036-3052.e5. https://doi.org/10.1016/j.neuron.2022.07.004

D'Addario, S. L., Di Segni, M., Ledonne, A., Piscitelli, R., Babicola, L., Martini, A., Spoleti, E., Mancini, C., Ielpo, D., D'Amato, F. R., Andolina, D., Ragozzino, D., Mercuri, N. B., Cifani, C., Renzi, M., Guatteo, E., & Ventura, R. (2021). Resilience to anhedonia-passive coping induced by early life experience is linked to a long-lasting reduction of Ih current in VTA dopaminergic neurons: Altered Ih current in the VTA of adult resilient-to-depression mice. *Neurobiology of Stress*, *14*. https://doi.org/10.1016/j.ynstr.2021.100324

D'Addario, S. L., Municchi, D., Mancini, C., Ielpo, D., Babicola, L., Di Segni, M., Iacono, L. Lo, Ferlazzo, F., Cifani, C., Andolina, D., & Ventura, R. (2023). The long-lasting effects of early life adversities are sex dependent: The signature of miR-34a. *Journal of Affective Disorders*, *322*, 277–288. https://doi.org/10.1016/j.jad.2022.11.035

De Franceschi, G., Vivattanasarn, T., Saleem, A. B., & Solomon, S. G. (2016). Vision Guides Selection of Freeze or Flight Defense Strategies in Mice. *Current Biology*, *26*(16), 2150–2154. https://doi.org/10.1016/j.cub.2016.06.006

De Gregorio, R., Pulcrano, S., De Sanctis, C., Volpicelli, F., Guatteo, E., von Oerthel, L., Latagliata, E. C., Esposito, R., Piscitelli, R. M., Perrone-Capano,

C., Costa, V., Greco, D., Puglisi-Allegra, S., Smidt, M. P., di Porzio, U., Caiazzo, M., Mercuri, N. B., Li, M., & Bellenchi, G. C. (2018). miR-34b/c Regulates Wnt1 and Enhances Mesencephalic Dopaminergic Neuron Differentiation. *Stem Cell Reports*, *10*(4), 1237–1250. https://doi.org/10.1016/j.stemcr.2018.02.006

De Kloet, E. R., & Molendijk, M. L. (2016). Coping with the Forced Swim Stressor: Towards Understanding an Adaptive Mechanism. In *Neural Plasticity* (Vol. 2016). Hindawi Limited. https://doi.org/10.1155/2016/6503162

Deakin, J. F. W., & Graeff, F. G. (1991). CRITIQUE: 5-HT and mechanisms of defence. *Journal of Psychopharmacology*, *5*(4), 305–315. https://doi.org/10.1177/026988119100500414

Devineni, A. V, & Scaplen, K. M. (2022). Neural Circuits Underlying Behavioral Flexibility: Insights From Drosophila. *Sec. Learning and Memory*. https://doi.org/10.3389/fn

Dias, B. G., Goodman, J. V., Ahluwalia, R., Easton, A. E., Andero, R., & Ressler, K. J. (2014). Amygdala-Dependent Fear Memory Consolidation via miR-34a and Notch Signaling. *Neuron*, *83*(4), 906–918. https://doi.org/10.1016/j.neuron.2014.07.019

Epigenetic landscape and miRNA involvement during neural crest development - Strobl-Mazzulla - 2012 . (n.d.).

Filipowicz, W., Bhattacharyya, S. N., & Sonenberg, N. (2008). Mechanisms of post-transcriptional regulation by microRNAs: Are the answers in sight? In *Nature Reviews Genetics* (Vol. 9, Issue 2, pp. 102–114). https://doi.org/10.1038/nrg2290

Fiori, E., Babicola, L., Andolina, D., Coassin, A., Pascucci, T., Patella, L., Han, Y. C., Ventura, A., & Ventura, R. (2015). Neurobehavioral Alterations in a Genetic Murine Model of Feingold Syndrome 2. *Behavior Genetics*, *45*(5), 547–559. https://doi.org/10.1007/s10519-015-9724-8

Fletcher, P. J., Ming, Z. H., & Higgins, G. A. (1993). Conditioned place preference induced by microinjection of 8-OH-DPAT into the dorsal or median raphe nucleus. *Psychopharmacology*, *113*(1), 31–36. https://doi.org/10.1007/BF02244330

Fonken, L. K., Gaudet, A. D., Gaier, K. R., Nelson, R. J., & Popovich, P. G. (2016). MicroRNA-155 deletion reduces anxiety- and depressive-like behaviors in mice. *Psychoneuroendocrinology*, *63*, 362–369. https://doi.org/10.1016/j.psyneuen.2015.10.019

Friedman, R. C., Farh, K. K. H., Burge, C. B., & Bartel, D. P. (2009). Most mammalian mRNAs are conserved targets of microRNAs. *Genome Research*, *19*(1), 92–105. https://doi.org/10.1101/gr.082701.108

Gheysarzadeh, A., Sadeghifard, N., Afraidooni, L., Pooyan, F., Mofid, M. R., Valadbeigi, H., Bakhtiari, H., & Keikhavani, S. (2018). Serum-based microRNA biomarkers for major depression: MiR-16, miR-135a, and miR-1202. *Journal of Research in Medical Sciences*, *23*(1). https://doi.org/10.4103/jrms.jrms_879_17

Gupta, P., Bhattacharjee, S., Sharma, A. R., Sharma, G., Lee, S.-S., & Chakraborty, C. (2017). miRNAs in Alzheimer Disease - A Therapeutic Perspective. *Current Alzheimer Research*, *14*(11). https://doi.org/10.2174/1567205014666170829101016

Gururajan, A., Naughton, M. E., Scott, K. A., O'Connor, R. M., Moloney, G., Clarke, G., Dowling, J., Walsh, A., Ismail, M. F., Shorten, G., Scott, L., McLoughlin, D. M., Cryan, J. F., & Dinan, T. G. (2016). MicroRNAs as biomarkers for major depression: A role for let-7b and let-7c. *Translational Psychiatry*, *6*(8). https://doi.org/10.1038/tp.2016.131

Ha, M., & Kim, V. N. (2014). Regulation of microRNA biogenesis. In *Nature Reviews Molecular Cell Biology* (Vol. 15, Issue 8, pp. 509–524). Nature Publishing Group. https://doi.org/10.1038/nrm3838

Haramati, S., Navon, I., Issler, O., Ezra-Nevo, G., Gil, S., Zwang, R., Hornstein, E., & Chen, A. (2011). MicroRNA as repressors of stress-induced anxiety: The case of amygdalar miR-34. *Journal of Neuroscience*, *31*(40), 14191–14203. https://doi.org/10.1523/JNEUROSCI.1673-11.2011

Harrison, A. A., Everitt, B. J., & Robbins, T. W. (1997). Central 5-HT depletion enhances impulsive responding without affecting the accuracy of attentional performance: Interactions with dopaminergic mechanisms. *Psychopharmacology*, *133*(4), 329–342. https://doi.org/10.1007/s002130050410

Hayashi, K., Nakao, K., & Nakamura, K. (2015). Appetitive and aversive information coding in the primate dorsal raphé nucleus. *Journal of Neuroscience*, *35*(15), 6195–6208. https://doi.org/10.1523/JNEUROSCI.2860-14.2015

He, M., Liu, Y., Wang, X., Zhang, M. Q., Hannon, G. J., & Huang, Z. J. (2012). Cell-Type-Based Analysis of MicroRNA Profiles in the Mouse Brain. *Neuron*, *73*(1), 35–48. https://doi.org/10.1016/j.neuron.2011.11.010

Hernández-Vázquez, F., Garduño, J., & Hernández-López, S. (2019). GABAergic modulation of serotonergic neurons in the dorsal raphe nucleus. *Reviews in the Neurosciences*, *30*(3), 289–303. https://doi.org/10.1515/revneuro-2018-0014

Homberg, J. R., & Contet, C. (2009). Deciphering the interaction of the corticotropin-releasing factor and serotonin brain systems in anxiety-related disorders. In *Journal of Neuroscience* (Vol. 29, Issue 44, pp. 13743–13745). https://doi.org/10.1523/JNEUROSCI.4362-09.2009

Honda, M., Kuwano, Y., Katsuura-Kamano, S., Kamezaki, Y., Fujita, K., Akaike, Y., Kano, S., Nishida, K., Masuda, K., & Rokutan, K. (2013). Chronic Academic Stress Increases a Group of microRNAs in Peripheral Blood. *PLoS ONE*, *8*(10). https://doi.org/10.1371/journal.pone.0075960

Hornung, J. P. (2003). The human raphe nuclei and the serotonergic system. *Journal of Chemical Neuroanatomy*, *26*(4), 331–343. https://doi.org/10.1016/j.jchemneu.2003.10.002

Hornung, J. P. (2010). The Neuronatomy of the Serotonergic System. In *Handbook of Behavioral Neuroscience* (Vol. 21, Issue C, pp. 51–64). https://doi.org/10.1016/S1569-7339(10)70071-0

Huang, K. W., Ochandarena, N. E., Philson, A. C., Hyun, M., Birnbaum, J. E., Cicconet, M., & Sabatini, B. L. (2019). Molecular and anatomical organization of the dorsal raphe nucleus. *ELife*, *8*. https://doi.org/10.7554/eLife.46464

Huang, L., Yuan, T., Tan, M., Xi, Y., Hu, Y., Tao, Q., Zhao, Z., Zheng, J., Han, Y., Xu, F., Luo, M., Sollars, P. J., Pu, M., Pickard, G. E., So, K. F., & Ren, C. (2017a). A retinoraphe projection regulates serotonergic activity and

looming-evoked defensive behaviour. *Nature Communications*, *8*. https://doi.org/10.1038/ncomms14908

Huang, L., Yuan, T., Tan, M., Xi, Y., Hu, Y., Tao, Q., Zhao, Z., Zheng, J., Han, Y., Xu, F., Luo, M., Sollars, P. J., Pu, M., Pickard, G. E., So, K. F., & Ren, C. (2017b). A retinoraphe projection regulates serotonergic activity and looming-evoked defensive behaviour. *Nature Communications*, *8*. https://doi.org/10.1038/ncomms14908

Inhibition of microRNA-34a Suppresses Epileptiform Discharges Through Regulating Notch Signaling and. (n.d.).

Jauhari, A., Singh, T., Singh, P., Parmar, D., & Yadav, S. (2018). Regulation of miR-34 Family in Neuronal Development. *Molecular Neurobiology*, *55*(2), 936–945. https://doi.org/10.1007/s12035-016-0359-4

Jin, Y., Luo, B., Su, Y. Y., Wang, X. X., Chen, L., Wang, M., Wang, W. W., & Chen, L. (2015). Sodium salicylate suppresses GABAergic inhibitory activity in neurons of rodent dorsal raphe nucleus. *PLoS ONE*, *10*(5). https://doi.org/10.1371/journal.pone.0126956

Johnson, P. L., Molosh, A. I., Federici, L. M., Bernabe, C., Haggerty, D., Fitz, S. D., Nalivaiko, E., Truitt, W., & Shekhar, A. (2019). Assessment of fear and anxiety associated behaviors, physiology and neural circuits in rats with reduced serotonin transporter (SERT) levels. *Translational Psychiatry*, *9*(1). https://doi.org/10.1038/s41398-019-0368-y

Kawai, H., Bouchekioua, Y., Nishitani, N., Niitani, K., Izumi, S., Morishita, H., Andoh, C., Nagai, Y., Koda, M., Hagiwara, M., Toda, K., Shirakawa, H., Nagayasu, K., Ohmura, Y., Kondo, M., Kaneda, K., Yoshioka, M., & Kaneko, S. (2022). Median raphe serotonergic neurons projecting to the interpeduncular nucleus control preference and aversion. *Nature Communications*, *13*(1). https://doi.org/10.1038/s41467-022-35346-7

Kenny, P. J. (2014). Epigenetics, microRNA, and addiction. *Dialogues in Clinical Neuroscience*, *16*(3), 335–344. https://doi.org/10.31887/dcns.2014.16.3/pkenny

Kirby, L. G., Pernar, L., Valentino, R. J., & Beck, S. G. (2003). Distinguishing characteristics of serotonin and non-serotonin-containing cells in the dorsal raphe nucleus: Electrophysiological and immunohistochemical studies. *Neuroscience*, *116*(3), 669–683. https://doi.org/10.1016/S0306-4522(02)00584-5

Kuang, W. H., Dong, Z. Q., Tian, L. T., & Li, J. (2018). MicroRNA-451a, microRNA-34a-5p, and microRNA-221-3p as predictors of response to antidepressant treatment. *Brazilian Journal of Medical and Biological Research*, *51*(7). https://doi.org/10.1590/1414-431x20187212

Lai, C. Y., Yu, S. L., Hsieh, M. H., Chen, C. H., Chen, H. Y., Wen, C. C., Huang, Y. H., Hsiao, P. C., Hsiao, C. K., Liu, C. M., Yang, P. C., Hwu, H. G., & Chen, W. J. (2011). MicroRNA expression Aberration as potential peripheral blood biomarkers for Schizophrenia. *PLoS ONE*, *6*(6). https://doi.org/10.1371/journal.pone.0021635

Lan, H., Lu, H., Wang, X., & Jin, H. (2015). MicroRNAs as potential biomarkers in cancer: Opportunities and challenges. In *BioMed Research International* (Vol. 2015). Hindawi Publishing Corporation. https://doi.org/10.1155/2015/125094

Land, B. B., Bruchas, M. R., Schattauer, S., Giardino, W. J., Aita, M., Messinger, D., Hnasko, T. S., Palmiter, R. D., & Chavkin, C. (2009). Activation of the

kappa opioid receptor in the dorsal raphe nucleus mediates the aversive effects of stress and reinstates drug seeking. *Proceedings of the National Academy of Sciences of the United States of America*, *106*(45), 19168–19173. https://doi.org/10.1073/pnas.0910705106

Latagliata, E. C., Puglisi-Allegra, S., Ventura, R., & Cabib, S. (2018). Norepinephrine in the medial pre-frontal cortex supports accumbens shell responses to a novel palatable food in food-restricted mice only. *Frontiers in Behavioral Neuroscience*, *12*. https://doi.org/10.3389/fnbeh.2018.00007

Latta, C. H., Brothers, H. M., & Wilcock, D. M. (2015). Neuroinflammation in Alzheimer's disease; A source of heterogeneity and target for personalized therapy. In *Neuroscience* (Vol. 302, pp. 103–111). Elsevier Ltd. https://doi.org/10.1016/j.neuroscience.2014.09.061

Lee, R. C., Feinbaum, R. L., & Ambros, V. (1993). The C. elegans heterochronic gene lin-4 encodes small RNAs with antisense complementarity to lin-14. *Cell*, *75*(5), 843–854. https://doi.org/10.1016/0092-8674(93)90529-Y

Lee, S. Y., Lu, R. B., Wang, L. J., Chang, C. H., Lu, T., Wang, T. Y., & Tsai, K. W. (2020). Serum miRNA as a possible biomarker in the diagnosis of bipolar II disorder. *Scientific Reports*, *10*(1). https://doi.org/10.1038/s41598-020-58195-0

Li, Y., Zhong, W., Wang, D., Feng, Q., Liu, Z., Zhou, J., Jia, C., Hu, F., Zeng, J., Guo, Q., Fu, L., & Luo, M. (2016). Serotonin neurons in the dorsal raphe nucleus encode reward signals. *Nature Communications*, *7*. https://doi.org/10.1038/ncomms10503

Li, Z., Wei, J.-X., Zhang, G.-W., Huang, J. J., Zingg, B., Wang, X., Tao, H. W., & Zhang, L. I. (n.d.). Corticostriatal control of defense behavior in mice induced by auditory looming cues. *Nature Communications*, *12*. https://doi.org/10.5281/zenodo.4319461

Lichtensteiger, W., Bassetti-Gaille, C., Rehrauer, H., Georgijevic, J. K., Tresguerres, J. A. F., & Schlumpf, M. (2021). Converging Effects of Three Different Endocrine Disrupters on Sox and Pou Gene Expression in Developing Rat Hippocampus: Possible Role of microRNA in Sex Differences. *Frontiers in Genetics*, *12*. https://doi.org/10.3389/fgene.2021.718796

Lieben, C. K. J., Steinbusch, H. W. M., & Blokland, A. (2006). 5,7-DHT lesion of the dorsal raphe nuclei impairs object recognition but not affective behavior and corticosterone response to stressor in the rat. *Behavioural Brain Research*, *168*(2), 197–207. https://doi.org/10.1016/j.bbr.2005.11.003

Liu, L., Liu, L., Shi, J., Tan, M., Xiong, J., Li, X., Hu, Q., Yi, Z., & Mao, D. (2016). MicroRNA-34b mediates hippocampal astrocyte apoptosis in a rat model of recurrent seizures. *BMC Neuroscience*, *17*(1). https://doi.org/10.1186/s12868-016-0291-6

Lo Iacono, L., Ielpo, D., Accoto, A., Di Segni, M., Babicola, L., D'Addario, S. L., Ferlazzo, F., Pascucci, T., Ventura, R., & Andolina, D. (2020). MicroRNA-34a Regulates the Depression-like Behavior in Mice by Modulating the Expression of Target Genes in the Dorsal Raphè. *Molecular Neurobiology*, *57*(2), 823–836. https://doi.org/10.1007/s12035-019-01750-2

Lo Iacono, L., Ielpo, D., Parisi, C., Napoli, G., Accoto, A., Di Segni, M., Babicola, L., D'Addario, S. L., Guzzo, S. M., Pascucci, T., Ventura, R., & Andolina, D. (2021). MicroRNA-34a regulates 5-HT2C expression in dorsal raphe and contributes to the anti-depressant-like effect of fluoxetine.

Neuropharmacology, *190*. https://doi.org/10.1016/j.neuropharm.2021.108559

Lopez, J. P., Lim, R., Cruceanu, C., Crapper, L., Fasano, C., Labonte, B., Maussion, G., Yang, J. P., Yerko, V., Vigneault, E., El Mestikawy, S., Mechawar, N., Pavlidis, P., & Turecki, G. (2014). MiR-1202 is a primate-specific and brain-enriched microRNA involved in major depression and antidepressant treatment. *Nature Medicine*, *20*(7), 764–768. https://doi.org/10.1038/nm.3582

Lugli, G., Torvik, V. I., Larson, J., & Smalheiser, N. R. (2008). Expression of microRNAs and their precursors in synaptic fractions of adult mouse forebrain. *Journal of Neurochemistry*, *106*(2), 650–661. https://doi.org/10.1111/j.1471-4159.2008.05413.x

Luo, M., Zhou, J., & Liu, Z. (2015). Reward processing by the dorsal raphe nucleus: 5-HT and beyond. In *Learning and Memory* (Vol. 22, Issue 9, pp. 452–460). Cold Spring Harbor Laboratory Press. https://doi.org/10.1101/lm.037317.114

Maffioletti, E., Tardito, D., Gennarelli, M., & Bocchio-Chiavetto, L. (2014). Micro spies from the brain to the periphery: New clues from studies on microRNAs in neuropsychiatric disorders. *Frontiers in Cellular Neuroscience*, *8*(MAR). https://doi.org/10.3389/fncel.2014.00075

Marcinkiewcz, C. A., Mazzone, C. M., D'Agostino, G., Halladay, L. R., Hardaway, J. A., Diberto, J. F., Navarro, M., Burnham, N., Cristiano, C., Dorrier, C. E., Tipton, G. J., Ramakrishnan, C., Kozicz, T., Deisseroth, K., Thiele, T. E., McElligott, Z. A., Holmes, A., Heisler, L. K., & Kash, T. L. (2016). Serotonin engages an anxiety and fear-promoting circuit in the extended amygdala. *Nature*, *537*(7618), 97–101. https://doi.org/10.1038/nature19318

Marinelli, S., Schnell, S. A., Hack, S. P., Christie, M. J., Wessendorf, M. W., & Vaughan, C. W. (2004). Serotonergic and nonserotonergic dorsal raphe neurons are pharmacologically and electrophysiologically heterogeneous. *Journal of Neurophysiology*, *92*(6), 3532–3537. https://doi.org/10.1152/jn.00437.2004

Matthiesen, M., Spiacci, A., & Zangrossi, H. (2017). Effects of chemical stimulation of the lateral wings of the dorsal raphe nucleus on panic-like defensive behaviors and Fos protein expression in rats. *Behavioural Brain Research*, *326*, 103–111. https://doi.org/10.1016/j.bbr.2017.03.006

McCall, M. N., Kim, M. S., Adil, M., Patil, A. H., Lu, Y., Mitchell, C. J., Leal-Rojas, P., Xu, J., Kumar, M., Dawson, V. L., Dawson, T. M., Baras, A. S., Rosenberg, A. Z., Arking, D. E., Burns, K. H., Pandey, A., & Halushka, M. K. (2017). Toward the human cellular microRNAome. *Genome Research*, *27*(10), 1769–1781. https://doi.org/10.1101/gr.222067.117

Meerson, A., Cacheaux, L., Goosens, K. A., Sapolsky, R. M., Soreq, H., & Kaufer, D. (2010). Changes in brain MicroRNAs contribute to cholinergic stress reactions. *Journal of Molecular Neuroscience*, *40*(1–2), 47–55. https://doi.org/10.1007/s12031-009-9252-1

Michelsen, K. A., Schmitz, C., & Steinbusch, H. W. M. (2007). The dorsal raphe nucleus-From silver stainings to a role in depression. In *Brain Research Reviews* (Vol. 55, Issue 2 SPEC. ISS., pp. 329–342). Elsevier. https://doi.org/10.1016/j.brainresrev.2007.01.002

Miyazaki, K. W., Miyazaki, K., Tanaka, K. F., Yamanaka, A., Takahashi, A., Tabuchi, S., & Doya, K. (2014). Optogenetic activation of dorsal raphe serotonin neurons enhances patience for future rewards. *Current Biology*, *24*(17), 2033–2040. https://doi.org/10.1016/j.cub.2014.07.041

Mohamed, H. A., Abdelkafy, A. E., Khairy, R. M. M., Abdelraheim, S. R., Kamel, B. A., & Marey, H. (2023). MicroRNAs and cytokines as potential predictive biomarkers for COVID-19 disease progression. *Scientific Reports*, *13*(1). https://doi.org/10.1038/s41598-023-30474-6

Nahand, J. S., Taghizadeh-boroujeni, S., Karimzadeh, M., Borran, S., Pourhanifeh, M. H., Moghoofei, M., Bokharaei-Salim, F., Karampoor, S., Jafari, A., Asemi, Z., Tbibzadeh, A., Namdar, A., & Mirzaei, H. (2019). microRNAs: New prognostic, diagnostic, and therapeutic biomarkers in cervical cancer. In *Journal of Cellular Physiology* (Vol. 234, Issue 10, pp. 17064–17099). Wiley-Liss Inc. https://doi.org/10.1002/jcp.28457

Navarro, F., & Lieberman, J. (2015). miR-34 and p53: New insights into a complex functional relationship. *PLoS ONE*, *10*(7). https://doi.org/10.1371/journal.pone.0132767

Ngeles Fernández-Gil, M., Palacios-Bote, R., Leo-Barahona, M., & Mora-Encinas, J. P. (2010). Anatomy of the brainstem: A gaze into the stem of life. *Seminars in Ultrasound, CT and MRI*, *31*(3), 196–219. https://doi.org/10.1053/j.sult.2010.03.006

Nishitani, N., Nagayasu, K., Asaoka, N., Yamashiro, M., Andoh, C., Nagai, Y., Kinoshita, H., Kawai, H., Shibui, N., Liu, B., Hewinson, J., Shirakawa, H., Nakagawa, T., Hashimoto, H., Kasparov, S., & Kaneko, S. (2019). Manipulation of dorsal raphe serotonergic neurons modulates active coping to inescapable stress and anxiety-related behaviors in mice and rats. *Neuropsychopharmacology*, *44*(4), 721–732. https://doi.org/10.1038/s41386-018-0254-y

Ogawa, S. K., Cohen, J. Y., Hwang, D., Uchida, N., & Watabe-Uchida, M. (2014). Organization of monosynaptic inputs to the serotonin and dopamine neuromodulatory systems. *Cell Reports*, *8*(4), 1105–1118. https://doi.org/10.1016/j.celrep.2014.06.042

Paquelet, G. E., Carrion, K., Lacefield, C. O., Zhou, P., Hen, R., & Miller, B. R. (2022). Single-cell activity and network properties of dorsal raphe nucleus serotonin neurons during emotionally salient behaviors. *Neuron*, *110*(16), 2664-2679.e8. https://doi.org/10.1016/j.neuron.2022.05.015

Patrono, E., Segni, M. Di, Patella, L., Andolina, D., Valzania, A., Latagliata, E. C., Felsani, A., Pompili, A., Gasbarri, A., Puglisi-Allegra, S., & Ventura, R. (2015). When chocolate seeking becomes compulsion: Gene-environment interplay. *PLoS ONE*, *10*(3). https://doi.org/10.1371/journal.pone.0120191

Peyron, C., Petit, J. M., Rampon, C., Jouvet, M., & Luppi, P. H. (1997). Forebrain afferents to the rat dorsal raphe nucleus demonstrated by retrograde and anterograde tracing methods. *Neuroscience*, *82*(2), 443–468. https://doi.org/10.1016/S0306-4522(97)00268-6

Pibiri, F., Nelson, M., Guidotti, A., Costa, E., & Pinna, G. (n.d.). *Decreased corticolimbic allopregnanolone expression during social isolation enhances contextual fear: A model relevant for posttraumatic stress disorder*.

Pollak Dorocic, I., Fürth, D., Xuan, Y., Johansson, Y., Pozzi, L., Silberberg, G., Carlén, M., & Meletis, K. (2014). A Whole-Brain Atlas of Inputs to

Serotonergic Neurons of the Dorsal and Median Raphe Nuclei. *Neuron*, *83*(3), 663–678. https://doi.org/10.1016/j.neuron.2014.07.002

Rea, K., Cremers, T. I. F. H., & Westerink, B. H. C. (2005). HPLC conditions are critical for the detection of GABA by microdialysis. *Journal of Neurochemistry*, *94*(3), 672–679. https://doi.org/10.1111/j.1471-4159.2005.03218.x

Ren, J., Friedmann, D., Xiong, J., Liu, C. D., Ferguson, B. R., Weerakkody, T., DeLoach, K. E., Ran, C., Pun, A., Sun, Y., Weissbourd, B., Neve, R. L., Huguenard, J., Horowitz, M. A., & Luo, L. (2018). Anatomically Defined and Functionally Distinct Dorsal Raphe Serotonin Sub-systems. *Cell*, *175*(2), 472-487.e20. https://doi.org/10.1016/j.cell.2018.07.043

Rompre, P. P., & Miliaressis, E. (1985). Pontine and mesencephalic substrates of self-stimulation. *Brain Research*, *359*(1–2), 246–259. https://doi.org/10.1016/0006-8993(85)91435-0

Rong, H., Liu, T. B., Yang, K. J., Yang, H. C., Wu, D. H., Liao, C. P., Hong, F., Yang, H. Z., Wan, F., Ye, X. Y., Xu, D., Zhang, X., Chao, C. A., & Shen, Q. J. (2011). MicroRNA-134 plasma levels before and after treatment for bipolar mania. *Journal of Psychiatric Research*, *45*(1), 92–95. https://doi.org/10.1016/j.jpsychires.2010.04.028

Samynathan, R., Venkidasamy, B., Shanmugam, A., Ramalingam, S., & Thiruvengadam, M. (2023). Functional role of microRNA in the regulation of biotic and abiotic stress in agronomic plants. In *Frontiers in Genetics* (Vol. 14). Frontiers Media SA. https://doi.org/10.3389/fgene.2023.1272446

Sargin, D., Jeoung, H. S., Goodfellow, N. M., & Lambe, E. K. (2019). Serotonin Regulation of the Prefrontal Cortex: Cognitive Relevance and the Impact of Developmental Perturbation. *ACS Chemical Neuroscience*, *10*(7), 3078–3093. https://doi.org/10.1021/acschemneuro.9b00073

Schwarzenbach, H., Nishida, N., Calin, G. A., & Pantel, K. (2014). Clinical relevance of circulating cell-free microRNAs in cancer. In *Nature Reviews Clinical Oncology* (Vol. 11, Issue 3, pp. 145–156). https://doi.org/10.1038/nrclinonc.2014.5

Sengupta, A., & Holmes, A. (2019a). A Discrete Dorsal Raphe to Basal Amygdala 5-HT Circuit Calibrates Aversive Memory. *Neuron*, *103*(3), 489-505.e7. https://doi.org/10.1016/j.neuron.2019.05.029

Sengupta, A., & Holmes, A. (2019b). A Discrete Dorsal Raphe to Basal Amygdala 5-HT Circuit Calibrates Aversive Memory. *Neuron*, *103*(3), 489-505.e7. https://doi.org/10.1016/j.neuron.2019.05.029

Seo, C., Guru, A., Jin, M., Ito, B., Sleezer, B. J., Ho, Y. Y., Wang, E., Boada, C., Krupa, N. A., Kullakanda, D. S., Shen, C. X., & Warden, M. R. (2019a). Intense threat switches dorsal raphe serotonin neurons to a paradoxical operational mode. *Science*, *363*(6426), 539–542. https://doi.org/10.1126/science.aau8722

Seo, C., Guru, A., Jin, M., Ito, B., Sleezer, B. J., Ho, Y. Y., Wang, E., Boada, C., Krupa, N. A., Kullakanda, D. S., Shen, C. X., & Warden, M. R. (2019b). Intense threat switches dorsal raphe serotonin neurons to a paradoxical operational mode. *Science*, *363*(6426), 539–542. https://doi.org/10.1126/science.aau8722

Shang, C., Chen, Z., Liu, A., Li, Y., Zhang, J., Qu, B., Yan, F., Zhang, Y., Liu, W., Liu, Z., Guo, X., Li, D., Wang, Y., & Cao, P. (2018). Cite this article

17k Accesses 112 Citations 17 Altmetric Metrics. In *Nature Communications* (Vol. 9).

Shin, R., & Ikemoto, S. (2010). The GABAB receptor agonist baclofen administered into the median and dorsal raphe nuclei is rewarding as shown by intracranial self-administration and conditioned place preference in rats. *Psychopharmacology*, *208*(4), 545–554. https://doi.org/10.1007/s00213-009-1757-3

Smalheiser, N. R., Lugli, G., Rizavi, H. S., Torvik, V. I., Turecki, G., & Dwivedi, Y. (2012). MicroRNA expression is down-regulated and reorganized in prefrontal cortex of depressed suicide subjects. *PLoS ONE*, *7*(3). https://doi.org/10.1371/journal.pone.0033201

Sohel, M. H. (2016). Extracellular/Circulating MicroRNAs: Release Mechanisms, Functions and Challenges. *Achievements in the Life Sciences*, *10*(2), 175–186. https://doi.org/10.1016/j.als.2016.11.007

Spoida, K., Masseck, O. A., Deneris, E. S., & Herlitze, S. (2014). Gq/5-HT2c receptor signals activate a local GABAergic inhibitory feedback circuit to modulate serotonergic firing and anxiety in mice. *Proceedings of the National Academy of Sciences of the United States of America*, *111*(17), 6479–6484. https://doi.org/10.1073/pnas.1321576111

Stuart, S. A., & Robinson, E. S. J. (2015). Reducing the stress of drug administration: Implications for the 3Rs. *Scientific Reports*, *5*. https://doi.org/10.1038/srep14288

Taylor, S. R., Kobayashi, M., Vilella, A., Tiwari, D., Zolboot, N., Du, J. X., Spencer, K. R., Hartzell, A., Girgiss, C., Abaci, Y. T., Shao, Y., De Sanctis, C., Bellenchi, G. C., Darnell, R. B., Gross, C., Zoli, M., Berg, D. K., & Lippi, G. (2023). MicroRNA-218 instructs proper assembly of hippocampal networks. *ELife*, *12*. https://doi.org/10.7554/eLife.82729

Themousebraininstereotaxiccoordinates. (n.d.).

Tuncdemir, S. N., Fishell, G., & Batista-Brito, R. (2015). MiRNAs are Essential for the Survival and Maturation of Cortical Interneurons. *Cerebral Cortex*, *25*(7), 1842–1857. https://doi.org/10.1093/cercor/bht426

Ventura, R., Latagliata, E. C., Morrone, C., La Mela, I., & Puglisi-Allegra, S. (2008). Prefrontal norepinephrine determines attribution of 'High' motivational salience. *PLoS ONE*, *3*(8). https://doi.org/10.1371/journal.pone.0003044

Wan, Y., Liu, Y., Wang, X., Wu, J., Liu, K., Zhou, J., Liu, L., & Zhang, C. (2015). Identification of differential microRNAs in cerebrospinal fluid and serum of patients with major depressive disorder. *PLoS ONE*, *10*(3). https://doi.org/10.1371/journal.pone.0121975

Wang, F., Flanagan, J., Su, N., Wang, L. C., Bui, S., Nielson, A., Wu, X., Vo, H. T., Ma, X. J., & Luo, Y. (2012). RNAscope: A novel in situ RNA analysis platform for formalin-fixed, paraffin-embedded tissues. *Journal of Molecular Diagnostics*, *14*(1), 22–29. https://doi.org/10.1016/j.jmoldx.2011.08.002

Wang, H. L., Zhang, S., Qi, J., Wang, H., Cachope, R., Mejias-Aponte, C. A., Gomez, J. A., Mateo-Semidey, G. E., Beaudoin, G. M. J., Paladini, C. A., Cheer, J. F., & Morales, M. (2019). Dorsal Raphe Dual Serotonin-Glutamate Neurons Drive Reward by Establishing Excitatory Synapses on VTA Mesoaccumbens Dopamine Neurons. *Cell Reports*, *26*(5), 1128-1142.e7. https://doi.org/10.1016/j.celrep.2019.01.014

Wang, S., Xiang, J., Li, Z., Lu, S., Hu, J., Gao, X., Yu, L., Wang, L., Wang, J., Wu, Y., Chen, Z., & Zhu, H. (2015). A plasma microRNA panel for early detection of colorectal cancer. *International Journal of Cancer*, *136*(1), 152–161. https://doi.org/10.1002/ijc.28136

Wang, Y., Medvid, R., Melton, C., Jaenisch, R., & Blelloch, R. (2007). DGCR8 is essential for microRNA biogenesis and silencing of embryonic stem cell self-renewal. *Nature Genetics*, *39*(3), 380–385. https://doi.org/10.1038/ng1969

Waselus, M., Valentino, R. J., & Van Bockstaele, E. J. (2011). Collateralized dorsal raphe nucleus projections: A mechanism for the integration of diverse functions during stress. In *Journal of Chemical Neuroanatomy* (Vol. 41, Issue 4, pp. 266–280). https://doi.org/10.1016/j.jchemneu.2011.05.011

Yang, T., Yu, K., Zhang, X., Xiao, X., Chen, X., Fu, Y., & Li, B. (2023). Plastic and stimulus-specific coding of salient events in the central amygdala. *Nature*, *616*(7957), 510–519. https://doi.org/10.1038/s41586-023-05910-2

Zhao, Y., Jaber, V. R., LeBeauf, A., Sharfman, N. M., & Lukiw, W. J. (2019). MicroRNA-34a (miRNA-34a) mediated down-regulation of the post-synaptic cytoskeletal element SHANK3 in sporadic Alzheimer's disease (AD). In *Frontiers in Neurology* (Vol. 10, Issue FEB). Frontiers Media S.A. https://doi.org/10.3389/fneur.2019.00028

Zhou, L., Liu, M. Z., Li, Q., Deng, J., Mu, D., & Sun, Y. G. (2017). Organization of Functional Long-Range Circuits Controlling the Activity of Serotonergic Neurons in the Dorsal Raphe Nucleus. *Cell Reports*, *18*(12), 3018–3032. https://doi.org/10.1016/j.celrep.2017.02.077

Zhou, Z., Liu, X., Chen, S., Zhang, Z., Liu, Y., Montardy, Q., Tang, Y., Wei, P., Liu, N., Li, L., Song, R., Lai, J., He, X., Chen, C., Bi, G., Feng, G., Xu, F., & Wang, L. (2019). A VTA GABAergic Neural Circuit Mediates Visually Evoked Innate Defensive Responses. *Neuron*, *103*(3), 473-488.e6. https://doi.org/10.1016/j.neuron.2019.05.027

Zurawek, D., Kusmider, M., Faron-Gorecka, A., Gruca, P., Pabian, P., Solich, J., Kolasa, M., Papp, M., & Dziedzicka-Wasylewska, M. (2017). Reciprocal MicroRNA Expression in Mesocortical Circuit and Its Interplay with Serotonin Transporter Define Resilient Rats in the Chronic Mild Stress. *Molecular Neurobiology*, *54*(8), 5741–5751. https://doi.org/10.1007/s12035-016-0107-9